

LaB-RAG: Label Boosted Retrieval Augmented Generation for Radiology Report Generation

Steven Song^{*,1,2}Anirudh Subramanyam^{*,3}Irene Madejski³Robert L. Grossman^{†,1,3,4}

Abstract

In the current paradigm of image captioning, deep learning models are trained to generate text from image embeddings of latent features. We challenge the assumption that these latent features ought to be high-dimensional vectors which require model fine tuning to handle. Here we propose Label Boosted Retrieval Augmented Generation (LaB-RAG), a text-based approach to image captioning that leverages image descriptors in the form of categorical labels to boost standard retrieval augmented generation (RAG) with pretrained large language models (LLMs). We study our method in the context of radiology report generation (RRG), where the task is to generate a clinician’s report detailing their observations from a set of radiological images, such as X-rays. We argue that simple linear classifiers over extracted image embeddings can effectively transform X-rays into text-space as radiology-specific labels. In combination with standard RAG, we show that these derived text labels can be used with general-domain LLMs to generate radiology reports. Without ever training our generative language model or image feature encoder models, and without ever directly “showing” the LLM an X-ray, we demonstrate that LaB-RAG achieves better results across natural language and radiology language metrics compared with other retrieval-based RRG methods, while attaining competitive results compared to other fine-tuned vision-language RRG models. We further present results of our experiments with various components of LaB-RAG to better understand our method. Finally, we critique the use of a popular RRG metric, arguing it is possible to artificially inflate its results without true data-leakage. Our code is available at: <https://github.com/uc-cdis/label-boosted-RAG-for-RRG>.

*These authors contributed equally

†Corresponding author: rgrossman1@uchicago.edu

¹Department of Computer Science, University of Chicago

²Medical Scientist Training Program, Pritzker School of Medicine

³Center for Translational Data Science, University of Chicago

⁴Department of Medicine, University of Chicago

Preprint. Under Review.

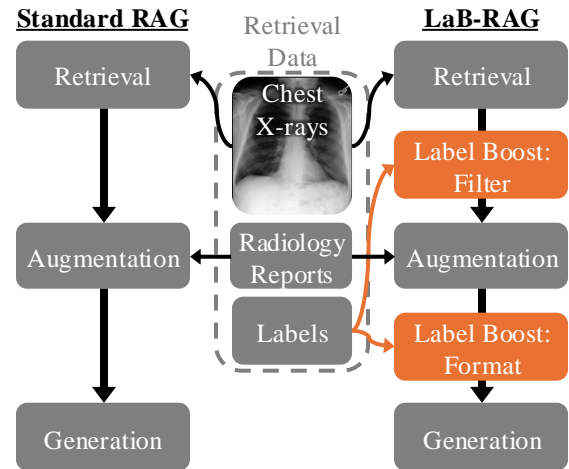


Figure 1. Overview of LaB-RAG for RRG.

1. Introduction

Radiology reports are free-text natural language notes describing the observations seen in radiological images, such as X-rays, CT scans, or MRI scans. These reports are written by board-certified radiologists, doctors who have had years of medical training to read these imaging modalities. This is a critically important task as radiological imaging provides a noninvasive view of internal organs and tissues, offering clinicians insights into how best to intervene and treat disease. However, the skills required to read these images can be highly specialized [67]; there is also an increasing demand for radiologists to read the growing number of images collected [13, 39, 66]. While remote radiology increased with the COVID-19 pandemic, these services still face challenges affecting the limited radiologist workforce [26]. Motivated by these considerations and coupled with the popularization of large language models (LLMs), there has been an increasing interest in developing AI tools to help bridge the gap for the radiologist shortage [24, 38, 52].

Radiology report generation (RRG) is the task of automatically generating these reports given the image [47, 69]. While RRG can be applied in any radiological imaging

modality, the most frequent modality studied in the literature is X-rays of the chest. This is likely due to the frequent and inexpensive collection of chest X-rays (CXRs) in the clinical setting and the public availability of paired chest X-ray and report datasets [69], such as MIMIC-CXR [35, 36], OpenI [14], PadChest [7], BIMCV-COVID19 [77], VinDr-CXR [55], and others. For CXRs, the task is typically formulated as generating the “Findings”, “Impression”, or both sections of the corresponding report [47]. Conceptually, the findings section describes all positive or negative observations seen in the X-ray, while the impression section summarizes and interprets those findings with recommendations for clinical diagnosis [59].

At its core, RRG is a form of image captioning, specialized for medical imaging [71]. In recent years, LLMs have demonstrated impressive performance across the medical domain, passing and excelling at US medical board exams and outperforming clinicians in certain tasks [11, 58, 68]. While these results do not translate directly to clinical viability, medical image captioning is a natural area of research application for such LLMs. Efforts typically involve fine-tuning vision-language models for the medical image modality of interest [1, 3]. Even when starting with a pre-trained language, vision, or multimodal foundation models (FMs), domain adaptation is typically expected when the task is specific and potentially out-of-distribution [6].

Model adaptation classically involves model training via supervised fine tuning (SFT). SFT of FMs is becoming increasingly difficult as models become larger, requiring compute resources greater than consumer-grade workstations can provide [75]. While parameter-efficient fine tuning (PEFT) methods have demonstrated competitive results [16], a form of LLM adaptation that does not require model training is in-context learning (ICL) [17]. The goal of ICL is to have an LLM infer the target output using examples of input-output pairs given jointly at inference time with the target input [49]. Related to ICL is retrieval augmented generation (RAG), a framework for providing additional context to an LLM prompt by retrieving documents related to the input query [42]. ICL and RAG can be combined to retrieve examples that are specific to the target input [19]. However, the standard approach for ICL and RAG uses text examples and inputs, whereas RRG is an image to text task.

While general domain vision-language FMs are improving even on medical vision-language tasks [48, 68], there are an increasing number of medical modality specific FMs which may offer better performance for tasks over these modalities [2, 4, 5, 10, 21, 23, 46, 51, 53, 74, 78, 80, 81]. It is an open area of research on how to compose together these FMs which were not necessarily jointly trained [9, 45]. Furthermore, the composition or adaptation method depends on the task. For image captioning, text generation must generally be informed by the image features. We ar-

Comparison	LaB-RAG	RAG	SFT
SOTA on clinical metrics	✓	✗	✓
No fine tuning of DL models	✓	✓	✗
Uses disjoint vision/text models	✓	✓	✗
Modular inference components	✓	✓	✗
Simple model ensemble	✓	✗	✗

Table 1. Conceptual comparison of LaB-RAG with other standard frameworks.

gue that the image features need not be high-dimensional latent or token embeddings, as in the current paradigm of multimodal LLMs.

We propose LaB-RAG, Label Boosted Retrieval Augmented Generation, a method for image captioning via RAG and ICL without the need to train any deep learning models. We study LaB-RAG in the context of RRG. Fig. 1 shows a visual overview of LaB-RAG compared to standard RAG. Tab. 1 includes a high-level conceptual comparison of LaB-RAG to standard RAG and SFT methods for RRG.

Main Contributions:

- **A generalizable framework to use classical machine learning (ML) to boost LLM performance.** By training simple ML models, *e.g.* logistic regression, to derive categorical labels from images, we propose to use the labels to inform RAG retrieval and to use the label names as textual image descriptors input to LLMs. This adapts from frozen pretrained vision models to frozen pretrained LLMs, only ever training classical models.
- **State of the art (SOTA) performance for RRG.** We show that LaB-RAG for RRG can achieve SOTA when compared with RRG models from the literature. We further experiment with and analyze effects of different components of LaB-RAG.
- **Critique of a commonly used RRG metric.** We critique the use of a label-based RRG metric commonly used in the literature, demonstrating that we can inflate its results by using its labels in LaB-RAG.

2. Related Work

As interest in RRG has steadily increased [69], there are an abundance of available RRG models from the literature trained to generate reports over CXRs. Additionally, the recent BioNLP workshop at ACL 2024 hosted a shared task on RRG [15] where several new models were presented. These published methods can be categorized by the report sections they generate, the “Findings” [73], “Impression” [18, 28, 54, 64, 65], both independently [12, 56], or both jointly [72]. Models from the literature can be further divided by the method for generation, either by a generative

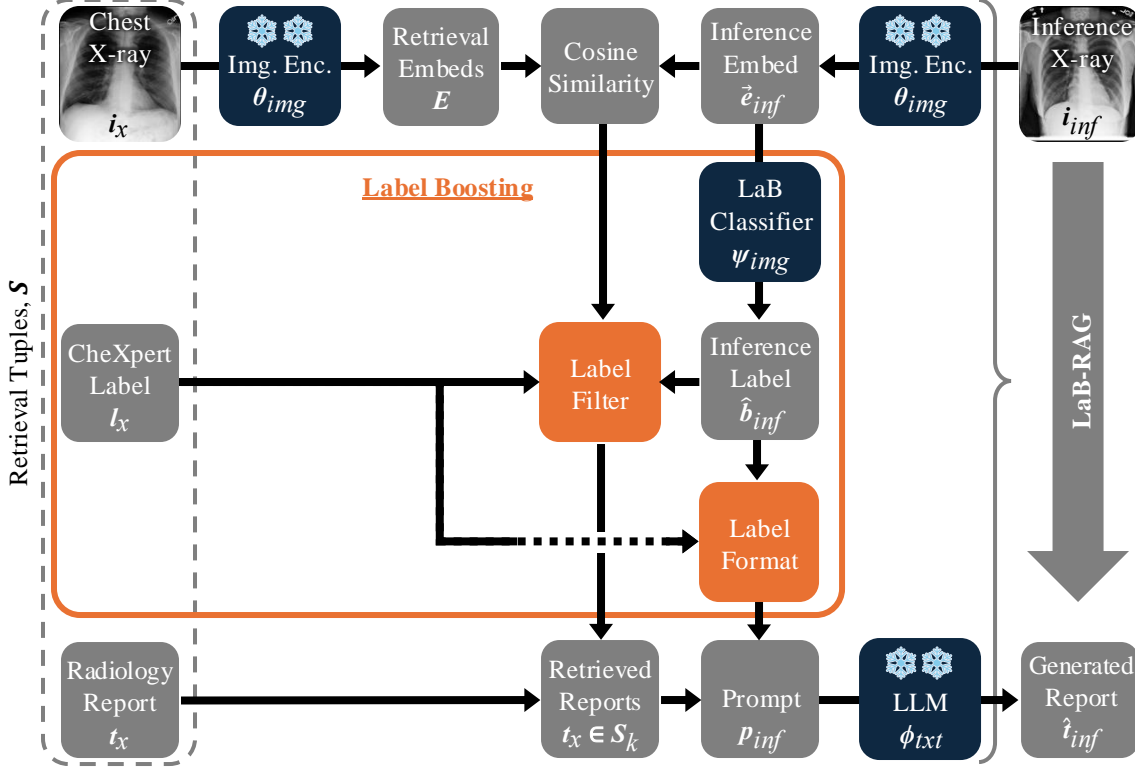


Figure 2. LaB-RAG inference for RRG. Symbols correspond to those in Alg. 1.

Algorithm 1 Pseudocode of LaB-RAG for RRG

- Require:** inference image i_{inf}
Require: retrieval studies with image-label-text tuples
 $S \leftarrow \{(i_x, l_x, t_x)\}$
Require: image embedding model θ_{img}
Require: text generative model ϕ_{txt}
- 1: compute inference embedding $\vec{e}_{inf} \leftarrow \theta_{img}(i_{inf})$
 - 2: compute retrieval embeddings
 $E \leftarrow [\dots, \vec{e}_x, \dots]^T, \vec{e}_x \leftarrow \theta_{img}(i_x)$
 - 3: binarize retrieval labels $B \leftarrow \{b_x \leftarrow l_x = 1\}$
 - 4: train image classification model $\psi_{img}(E) \rightarrow B$
 - 5: infer inference image label $\hat{b}_{inf} \leftarrow \psi_{img}(\vec{e}_{inf})$
 - 6: compute image cosine similarity
 $\vec{d} \leftarrow [\dots, d_x, \dots], d_x \leftarrow (\vec{e}_{inf} \cdot \vec{e}_x) / \|\vec{e}_{inf}\| \|\vec{e}_x\|$
 - 7: sort studies by similarity $\vec{r} \leftarrow [\dots, s_x, \dots], d_x \geq d_{x+1}$
 - 8: **Label Filter:** filter or rerank $s_x \in \vec{r}$ by comparing $b_x \in B$ and \hat{b}_{inf} (multiple possible filters)
 - 9: retrieve studies S_k of the k highest ranked samples in \vec{r}
 - 10: prepare prompt p_{inf} using $t_x \in S_k$
 - 11: **Label Format:** format prompt p_{inf} with retrieved labels $l_x \in S_k$, and \hat{b}_{inf} (multiple possible formats)
 - 12: generate report $\hat{t}_{inf} \leftarrow \phi_{txt}(p_{inf})$
-

LLM conditioned only on image features [12, 54, 56, 73] or by text retrieval and processing [18, 28, 54, 64, 65, 72].

There are two primary ways by which LLMs are fine-tuned to generate the report based on input CXR embeddings. CXRMate [56] is trained with image embeddings input via cross attention [8, 44, 76]. CheXagent [12] and RGRG [73] are instead trained with image embeddings prepended as input tokens before the report, adapting the image embeddings into token embedding space.

The following retrieval-based methods use cross-modal image-to-text retrieval, requiring training of a retrieval model with a joint embedding space for CXRs and their corresponding reports. CXR-RePaiR-Gen [65] leverages CXR-ReDonE [64] for its cross-modal retrieval models and otherwise is the closest implementation of a standard RAG pipeline. FactMM-RAG [72] also employs RAG for inference, but trains its own retrieval model using RadGraph [27] labels to inform the joint embedding space. This is broadly similar to the training of X-REM’s [28] retrieval model, however X-REM uses CheXbert [70] labels. X-REM outputs a concatenation of retrieved text as the final report. CXR-RePaiR [18] also uses concatenation of retrieved text for its final output, however its retrieval model is trained via the basic CLIP [62] method. CXR-ReDonE [64] is the same as CXR-RePaiR except the training/retrieval data was cleaned to remove “priors” indicating a previous CXR [63].

The most closely related method compared to LaB-RAG is Pragmatic Retrieval/Llama [54]. Like LaB-RAG, Pragmatic derives categorical labels directly from the CXR. However, Pragmatic trains an end-to-end ResNet50 [22] model, whereas LaB-RAG uses simpler logistic classifiers trained over extracted image embeddings. Additionally, Pragmatic requires the report’s “Indication”, the clinical reason and motivation for the imaging study. While LaB-RAG uses both image embedding similarity and label matching for retrieval, Pragmatic Retrieval only uses label matching of image and indication for retrieval of report text. Pragmatic Retrieval then concatenates label-retrieved text as the final report. Pragmatic Llama does no retrieval, instead training an LLM to generate the report given the indication text and the positive image labels as text. LaB-RAG also uses labels as textual image descriptors but relies on ICL and model instructing, and thus does not require model fine-tuning.

3. LaB-RAG Framework

LaB-RAG uses a label boosted RAG algorithm with ICL to do image captioning. LaB-RAG retrieves paired example text using image embedding similarity. Retrieved texts are then fed into a general domain LLM with strong instruction following and natural language comprehension capabilities. **We improve upon standard RAG by incorporating predicted categorical labels into both the example retrieval and text augmentation steps.** The overview of LaB-RAG applied to RRG is presented in Fig. 2 with its high-level pseudocode described in Alg. 1. We evaluate our generation results against ground truth radiology reports using natural language metrics and clinical radiology language metrics. We compare our method against models from literature and against variations of our method.

3.1. Image, Text, and Label Dataset

For our study, we use chest X-rays, radiology reports, CheXpert [25] labels, metadata, and data splits from MIMIC-CXR v2.1.0 and its related datasets. [32, 33, 35, 36]. The dataset is split at the patient level. The final number of samples used in each of our experiments depends on the availability of all required data modalities. Further details on the dataset are provided in Sec. S2.

Because the radiology reports are written at the study level and the CheXpert [25] labeler derives labels from the report, the categorical labels are also defined per study. In order of preference, CheXpert labels are extracted from the “Impression”, “Findings”, or last paragraph sections of the report [32]. CheXpert provides 14 labels where each label describes a radiological observation, including “No Finding”. Each label gets a value of 1 (positive), 0 (negative), -1 (uncertain), or null (unmentioned). A report receives a multilabel classification where any combination of labels and

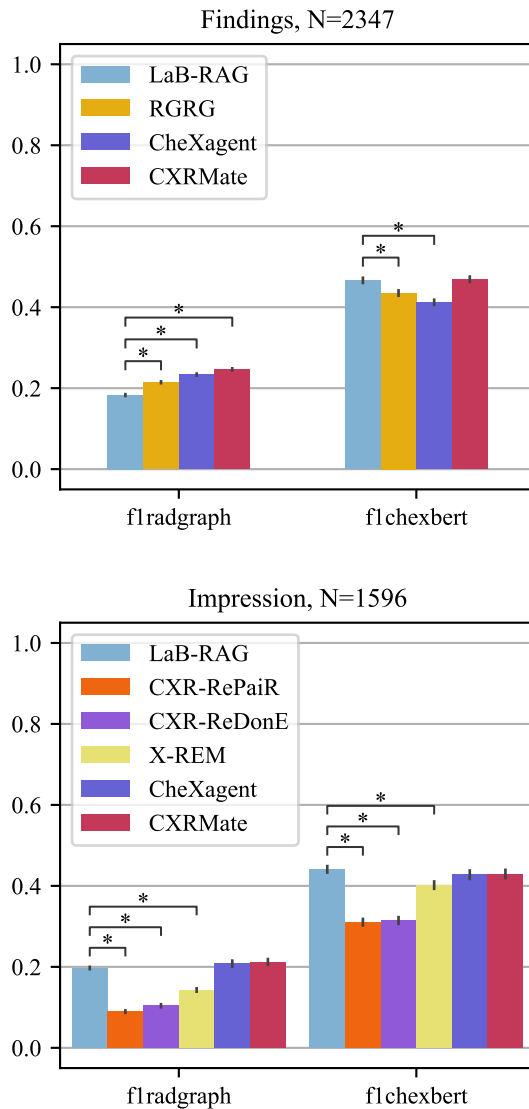


Figure 3. LaB-RAG does better than other retrieval methods (CXR-RePaiR/ReDonE, X-REM) and no different than SFT methods on “Impression” generation (CheXagent, CXRMate) and comparable to “Findings” generation measured by F1CheXbert (RGRG, CheXagent, CXRMate). See Sec. 5.3 for analysis of F1RadGraph results for “Findings” generation.

values can be assigned. It is thus possible to have a study with no positive labels; in such cases, we assign a positive “Other” label which is negative in all other instances. Our final labels are sets of 15 labels per study.

3.2. Image Feature Extraction

We compute image feature embeddings to train our image classifier and to enable retrieval of visually similar images and their associated text. For CXR data, we use the pre-

trained X-ray image encoder of BioViL-T [2] to extract image features. We select BioViL-T as our image encoder because it was trained over MIMIC-CXR, it achieved impressive performance on tasks via linear probing, and because the `hi-ml-multimodal` v0.2.2 python package made it simple to integrate the model into our code. While the joint vision-language training may have helped BioViL-T learn more meaningful embeddings for downstream tasks, LaB-RAG is agnostic to the method by which the image encoder was trained. Specifically, we extract X-ray embeddings with the frozen image-encoder of BioViL-T. For image-based retrieval, we use projected 128d embeddings; for training our image classifier, we use unprojected 512d embeddings.

3.3. Training LaB-Classifiers for Label Prediction

Because the CheXpert [25] labels are computed using the radiology report, using these labels of the target X-ray in the generation of its corresponding report constitutes a form of data-leakage. **We train a set of logistic regression models, LaB-Classifiers, on frozen image embeddings to classify images directly**, thereby preventing this leakage (Fig. S1). Further LaB-Classifier training details are in Sec. S3.

3.4. Label Boosted RAG Algorithm

To generate captions from images, LaB-RAG uses RAG with retrieved example text for ICL. We enhance both retrieval and augmentation steps using categorical labels describing the images and their corresponding text. Given an image at inference time, we rank the similarity of the inference image with all retrieval images in image embedding space (Fig. 2 Top). We apply label-based logic to filter or rerank the similarity scores (Fig. 2 Middle), described in Sec. 3.4.1. We retrieve the corresponding text of the highest ranked images, augment a prompt with the retrieved examples, and autoregressively generate a caption using a pre-trained LLM (Fig. 2 Bottom). We additionally incorporate labels in the prompt formatting step (Fig. 2 Middle), described in Sec. 3.4.2. See Alg. 1 for pseudocode.

For RRG, LaB-RAG by default uses BioViL-T [2] projected image embeddings, an “Exact” label filter, the top-5 ranked examples, the “Simple” label format and prompt, and Mistral-7B-Instruct-v0.3 [50]. For generation, we serve the LLM using vLLM [40] and do greedy decoding up to 512 tokens. In all experiments, we use the training and validation splits of our data as our retrieval set and do inference over the test split. **Given a retrieval corpus of the target report section, LaB-RAG is able to generate any arbitrary section**; however, depending on the radiology report section(s) we aim to generate and compare with, we filter the retrieval and inference sets to only studies with the target section.

3.4.1. Label Boosted Filtering

LaB-RAG does binary label matching to filter or rerank the ranked list of retrieval samples. LaB-RAG’s label boosting module takes an input list of samples, ranked by image similarity to the inference image, and outputs a ranked list of samples (Alg. 1 Step 8). We present three variations of this module. The simplest variant is “No-filter”, where we do not perform label-based filtering or reordering.

“Exact” filtering requires that every retrieved sample has the same binary labels as the inference image’s labels:

$$\begin{aligned} \text{filter}_{\text{exact}}(\vec{r}) &= [\dots, s_x, \dots] \\ b_x &= \hat{b}_{inf} \end{aligned} \quad (1)$$

where \vec{r} is a list of samples s sorted with most relevant samples at the beginning of the list, b_x is the binary label set of a sample s_x , and \hat{b}_{inf} is inference image’s inferred binary label set. This filtering will most often result in a shorter list than the input \vec{r} and it is possible that the output will be an empty list if the inferred label does not match any labels in the retrieval set (*e.g.* if the inferred label is unrealistic: both positive “No Finding” and “Atelectasis” in the context of RRG).

“Partial” filtering relaxes the constraint of the exact filter by re-sorting the retrieved samples based on the amount of overlapping positive labels between each sample’s label and the inferred image label:

$$\begin{aligned} \text{filter}_{\text{partial}}(\vec{r}) &= [\dots, s_x, \dots] \\ f(b_x) &\geq f(b_{x+1}) \\ \text{idx}_{\vec{r}}(s_x) &< \text{idx}_{\vec{r}}(s_{x+1}) \\ \hookrightarrow \text{if } f(b_x) &= f(b_{x+1}) \end{aligned} \quad (2)$$

where \vec{r} , s_x , b_x , and \hat{b}_{inf} are the same as above, and $f(b) = |b \wedge \hat{b}_{inf}|$ gives the amount of positive label overlap. The second condition ensures a stable reordering of \vec{r} , such that two samples with the same number of overlapping positive labels retain their relative position from image similarity. Notably, the number of overlapping positive labels does not depend on which labels overlap, nor does it consider the number of overlapping negative labels. This means that two samples with the same number of positive labels overlapped with the image labels can have different labels compared to each other and any sample may have more or less total positive labels compared with the image labels. For the “Partial” filter, the output list will always be the same length as the input.

3.4.2. Label Boosted Formatting and Prompts

LaB-RAG uses categorical label names as textual image descriptors for image captioning. It does so by formatting the

labels as text in the prompt for both the text examples and the inference image. Because the label formatting is intricately associated with the prompt structure, we include the description of our prompts here. In the context of RRG, each CheXpert [25] label is a 14 multiclass multilabel with a 15th binary class label of exclusion (our “Other” label). We thus present four label format and prompt combinations varying the degree of label verbosity and label type description and instruction. The “Naive” prompt does not utilize label descriptors and is closest to a standard RAG prompt with some model instructions.

The “Simple” prompt formats positive labels as a comma separated list before each example of text. It additionally applies the label formatting to the predicted labels of the inference image and appends this label text to the end of the prompt to condition the generation of the image’s report; the instructions within the prompt include minimal further details describing the label.

The “Verbose” prompt additionally includes all label values (negative, uncertain, and unmentioned for CheXpert labels) and expands the model instructions to describe these value types. The prompt does not describe the labels themselves. The “Instruct” prompt uses the exact same template as “Verbose” but adds explicit instructions on how to handle each value type. As the predicted image labels are binary positive or negative, the label set for the inference image will never have labels listed under other values. We refer the reader to Sec. S5 for the examples of the exact prompts and label formats.

4. Evaluation Strategy

To evaluate and compare LaB-RAG, we adopt RRG-specific metrics, F1-RadGraph [27] and F1-CheXbert [70]. These measure clinical relevance by computing the F1-score between clinical annotations of the actual and generated reports. The CheXbert annotations are the binarization of the 14 CheXpert [25] labels, while RadGraph annotations are broader in scope. We use the `radgraph` v0.1.12 and `flchexbert` v0.0.2 python packages for their implementations of RadGraph and CheXbert. We also measure natural language metrics, using `huggingface evaluate` v0.4.2 to compute BLEU-4 [60], ROUGE-L [43], and BERTScore [82]. We refer the reader to our code and Sec. S4 for our specific usage of these metrics.

4.1. Comparison to Literature Models

We compare against both retrieval-based (CXR-RePaiR [18], CXR-ReDonE [64], X-REM [28]) and direct latent image embedding tuned models (CXRMate [56, 57], CheX-agent [12], RGRG [73]). For CXRMate, we specifically use the version submitted to the BioNLP workshop [15, 57]. As each method may have slightly different filtering strategies for data preprocessing, we evaluate on the intersection of

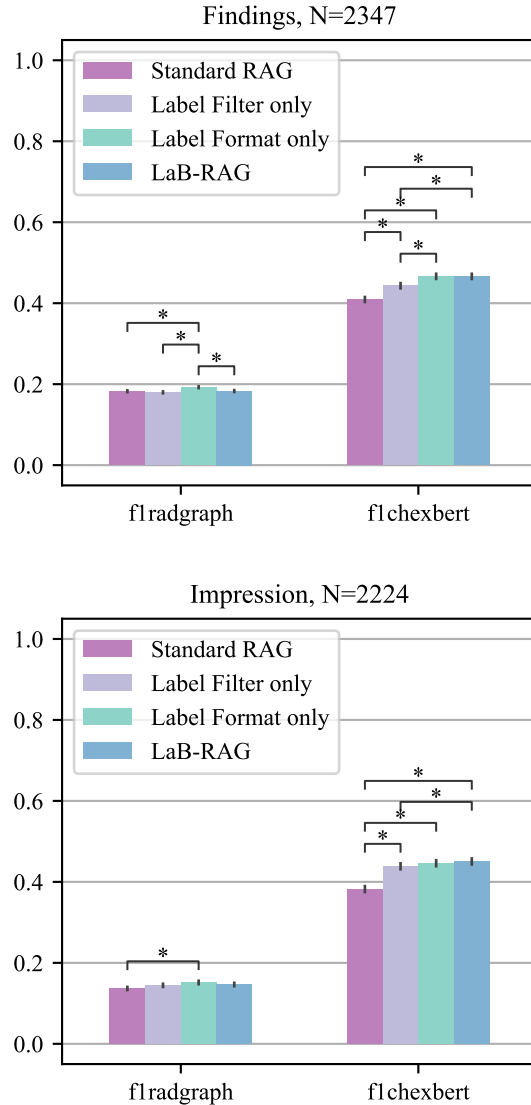


Figure 4. Comparison of simple individual label boosting components of LaB-RAG. Compared to SFT methods (Fig. 3), we attain a comparable $\sim 5\%$ improvement in F1CheXbert using minimal additional computation over standard RAG.

the test data splits for each method. LaB-RAG’s data preprocessing only requires there be a ground truth reference text to compare against, thus our test split is a superset of other methods’ test splits. More detailed descriptions of preparing and running each method from the literature are presented in Sec. S6.

As discussed in Sec. 2, RRG models can be categorized by the report section they generate. LaB-RAG is able to generate any target section given a corresponding retrieval corpus and thus comparison to other models only depend on code and data availability. We report results on generated

“Findings”, “Impression”, and the concatenation of these sections generated independently. All comparison models were trained in-part over MIMIC-CXR [35].

FactMM-RAG [72] and CXR-RePaiR-Gen [65] are also retrieval based methods, however they do not share code. While BioViL-T [2] and BioViL [4] report RRG metrics and are usable as encoders, they do not share code for autoregressive or precise retrieval based generation. Finally, the only missing component of Pragmatic Retrieval/Llama [54] is code to extract the required indication section. As the MIMIC Code Repository [34] requires modification to extract indications, we are unable to exactly replicate Pragmatic’s precise method.

5. Studies and Experiments on LaB-RAG

In the following sections, we present results and analyses of our studies on LaB-RAG. These include comparisons of LaB-RAG to literature models and experiments on varying components of our framework. Tab. S10 is a full table of our results across all metrics, models, and experiments. We discuss limitations and next steps where relevant.

5.1. Baseline Comparisons

We consider models from the literature as our baseline. For models which we could compare against that generate the “Findings” section, none are retrieval based. On “Findings” generation (Fig. 3 Top), LaB-RAG does comparable to SFT methods (RGRG [73], CheXagent [12], CXRMate [57]) on F1CheXbert, however underperforms in F1RadGraph. Yet on “Impression” generation (Fig. 3 Bottom), LaB-RAG is not significantly worse than any SFT method (CheXagent, CXRMate) and outperforms previous retrieval-based methods (CXR-RePaiR [18], CXR-ReDonE [64], X-REM [28]). Across natural language metrics (Fig. S3), differences in performance, while statistically significant, are small in magnitude (Tab. S10).

5.2. Variations of LaB-RAG

We experiment with the core label-boosting components of LaB-RAG and other modular components. Full results across all metrics are available in Sec. S7.

Label Filter and Format Effects. We first consider the simplest strategies for using labels, either “Exact” label match filtering or “Simple” positive label formatting. We show that inclusion of labels marginally changes F1RadGraph results while improving F1CheXbert performance by $\sim 5\%$ over standard RAG for both “Findings” and “Impression” (Fig. 4). A comparable gain in performance from the literature between CheXagent [12] and CXRMate [57] on “Findings” generation (Fig. 3 Top) required complex new training strategies and additional datasets. As previously observed, LaB-RAG is also comparable to

Actual	AP view of the chest. Right PICC (supp. dev.) is seen with tip at the upper SVC . Relatively low lung volumes are seen. The lungs however remain clear without consolidation, effusion or pulmonary vascular congestion . Cardiac silhouette appears moderately enlarged (cardiomegaly) , likely accentuated due to low lung volumes and AP technique.
LaB-RAG	In comparison with the previous radiograph, there is little change in the appearance of the heart and lungs . Cardiac silhouette is mildly prominent (cardiomegaly) and there is dense calcification within the aortic arch and descending portion . Blunting of the costophrenic angle is again seen, but no evidence of acute focal pneumonia or vascular congestion . Multiple triple-lumen catheter (supp. dev.) extends to the right atrium .
CXRMate	Single portable view of the chest was compared to previous exam from _____. Right-sided PICC (supp. dev.) is seen with tip in the upper SVC . The lungs are clear of focal consolidation or pulmonary vascular congestion . The cardiac silhouette is enlarged (cardiomegaly) but stable in configuration . There is no large pleural effusion . There is no pneumothorax . Osseous and soft tissue structures are unremarkable.

Table 2. Example “Findings” section demonstrating overvaluation by F1CheXbert. **Blue** entities are annotated with their corresponding CheXbert `label` and are also extracted by RadGraph. **Red** entities are only extracted by RadGraph. Despite CXRMate attaining higher F1RadGraph than LaB-RAG (0.6 vs 0.2) on this example, LaB-RAG matches CXRMate in F1CheXbert (both 1.0) due to LaB-RAG’s usage of labels.

CXRMate in absolute measures. For LaB-RAG, we attain this improvement over standard RAG with minimal additional computation, only requiring “Simple” label formatting; however we do not observe a meaningful improvement when adding “Exact” label filtering to “Simple” formatting, the default LaB-RAG settings. We hypothesize that this is because the LLM is able to infer which parts of the example reports are useful to describe those labels.

To test this, we present inexact label matched examples to the LLM by using our “Partial” label filter (Sec. 3.4.1). Fig. S5 shows that with the default “Simple” prompt, the filters are not meaningfully different in performance. We confirm that inexactly labeled examples are selected by examining the image similarity rank of the filtered selections. In Fig. S10, we observe the “Exact” filter selects fewer than the “Partial” filter of the most visually similar examples.

Thus the “Partial” filter will present more mismatched labels to the LLM, yet the stable performance implies the language model is attending to only relevant parts of the examples. Ultimately, given the “Exact” label filter’s improvement over standard RAG and the lack of detriment for the “Simple” label format, we use both label boosting components as defaults for LaB-RAG, aiming to potentially make it simpler for the LLM to parse high-quality label-matched text in the prompt.

Related to prompt complexity, we find that increasing the verbosity of the label format beyond positive labels with the “Simple” prompt tends to decrease performance (Fig. S6).

Image and Language Model Choice. As LaB-RAG is a fully modular framework, we analyze the choice of our pretrained models. We first compare comparable Mistral 7B LLMs: Instruct-v0.1 [29], BioMistral (Instruct-v0.1 further pretrained on PubMed Central) [41], and Instruct-v0.3 [50]. Fig. S7 shows that newer model versions improve RRG performance, while biomedical domain adaptation may be detrimental. This is contrary to previous literature [21] on biomedical domain adaptation, leading us to hypothesize that for a language-intensive approach (ICL), natural language capabilities may be more important than domain specific knowledge. One next step would be to test an LLM with domain-specific instruction following capabilities.

Additionally, the choice of image model directly impacts our label quality. We simulate the effect of using higher accuracy labels by using ground truth labels. We show in Fig. S8 that using true labels improves performance across the board, particularly in impression generation. The gap between LaB-Classifier predicted and true labels (Fig. S2) may be explained by Fig. S10, as image embedding similarity does not necessarily align with the CheXpert [25] labels. A natural extension may be to repeat our experiments with different pretrained image encoders or label sets.

Joint Section Evaluation. Finally, we experiment with modular retrieval examples. Given concatenations of the “Findings” and “Impression” for retrieval, LaB-RAG can jointly generate both sections. We compare this against performance of generating sections independently for studies which have both sections (Fig. S9 Top), showing that LaB-RAG does marginally better when generating jointly. We also compare against CheXagent [12] and CXRMate [57] by evaluating the concatenation of sections each method generates independently (Fig. S9 Bottom). We find a similar result to Fig. S3, where LaB-RAG is comparable to these methods in F1CheXbert but not on other metrics.

5.3. Extended Analyses

Motivated by the results comparing LaB-RAG to literature (Fig. 3), we sought to analyze why we were comparable to SOTA in F1RadGraph for “Impression” generation but not “Findings” generation. Tab. 2 includes an example of an

actual “Findings” section and its corresponding generations by LaB-RAG and CXRMate [57]. We annotate the entities identified by CheXbert [70] with their label. These entities are also identified by RadGraph [27], which also identifies many more. Examining RadGraph annotations, we observe that the entities of the actual report more closely align with those of CXRMate’s generation, hence the F1RadGraph achieved for CXRMate was 0.6 vs Lab-RAG’s 0.2. However, we also observe that the computed CheXbert labels of both LaB-RAG and CXRMate exactly match those of the actual report, resulting in F1CheXbert of 1.0.

We argue that F1CheXbert overvalues these generated “Findings” because it relies solely on 14 labels that describe disease related findings. This is most relevant to novel composite RRG metrics, such as RadCliQ [79], which include CheXbert as a component metric. As LaB-RAG explicitly uses these same labels in its label filter and format, we effectively ensure that these labels will be present in the generated report. This may also be the reason for LaB-RAG’s improved F1RadGraph performance in “Impression” generation. Since the “Impression” describes summary diagnoses, CheXbert and RadGraph entities may be more closely aligned with each other. It is thus an open question of which label set to use for label boosting. An interesting possibility may be using RadGraph derived labels.

5.4. Other Limitations

Though we make no claim of LaB-RAG’s clinical viability, an analysis of hallucinations is an important step towards this discussion for any model; Tab. 2 certainly shows hallucinations in both generations. Another potential limitation arises from the CheXpert [25] labels included by MIMIC-CXR-JPG [32]; these labels were derived on mixed report sections, however we do not consider their source for our section-specific generation. Lastly, a limitation of all methods using pretrained LLMs is the difficulty of detecting data leakage from pretraining over unknown training data.

6. Conclusion

In this work, we present LaB-RAG: a modular framework for image captioning using pretrained models. We study and analyze LaB-RAG in the context of RRG, showing that it achieves SOTA on clinical language metrics. We offer insights into the importance of different components of LaB-RAG, while also critiquing a widely used RRG metric, arguing we can inflate its results. Throughout our experiments, we stress the simplicity of LaB-RAG as an ensemble of frozen DL models boosted by classical linear models. The key to LaB-RAG is leveraging categorical labels as natural descriptors of images. Doing so enables LaB-RAG to use off-the-shelf models which do not need to be jointly trained, a task which requires large paired datasets. This enables LaB-RAG to be fully modular and flexible for users.

References

- [1] Hareem Ayesha, Sajid Iqbal, Mehreen Tariq, Muhammad Abrar, Muhammad Sanaullah, Ishaq Abbas, Amjad Rehman, Muhammad Farooq Khan Niazi, and Shafiq Hussain. Automatic medical image interpretation: State of the art and future directions. *Pattern Recognition*, 114:107856, 2021. 2
- [2] Shruthi Bannur, Stephanie Hyland, Qianchu Liu, Fernando Perez-Garcia, Maximilian Ilse, Daniel C Castro, Benedikt Boecking, Harshita Sharma, Kenza Bouzid, Anja Thieme, et al. Learning to exploit temporal structure for biomedical vision-language processing. In *Proceedings of the IEEE/CVF Conference on Computer Vision and Pattern Recognition*, pages 15016–15027, 2023. 2, 5, 7
- [3] Djamila-Romaissa Beddiar, Mourad Oussalah, and Tapio Seppänen. Automatic captioning for medical imaging (mic): a rapid review of literature. *Artificial intelligence review*, 56(5):4019–4076, 2023. 2
- [4] Benedikt Boecking, Naoto Usuyama, Shruthi Bannur, Daniel C Castro, Anton Schwaighofer, Stephanie Hyland, Maria Wetscherek, Tristan Naumann, Aditya Nori, Javier Alvarez-Valle, et al. Making the most of text semantics to improve biomedical vision–language processing. In *European conference on computer vision*, pages 1–21. Springer, 2022. 2, 7, 9
- [5] Elliot Bolton, Abhinav Venigalla, Michihiro Yasunaga, David Hall, Betty Xiong, Tony Lee, Roxana Daneshjou, Jonathan Frankle, Percy Liang, Michael Carbin, et al. Biomedlm: A 2.7 b parameter language model trained on biomedical text. *arXiv preprint arXiv:2403.18421*, 2024. 2
- [6] Rishi Bommasani, Drew A Hudson, Ehsan Adeli, Russ Altman, Simran Arora, Sydney von Arx, Michael S Bernstein, Jeannette Bohg, Antoine Bosselut, Emma Brunskill, et al. On the opportunities and risks of foundation models. *arXiv preprint arXiv:2108.07258*, 2021. 2
- [7] Aurelia Bustos, Antonio Pertusa, Jose-Maria Salinas, and Maria De La Iglesia-Vaya. Padchest: A large chest x-ray image dataset with multi-label annotated reports. *Medical image analysis*, 66:101797, 2020. 2
- [8] Chun-Fu Richard Chen, Quanfu Fan, and Rameswar Panda. Crossvit: Cross-attention multi-scale vision transformer for image classification. In *Proceedings of the IEEE/CVF international conference on computer vision*, pages 357–366, 2021. 3
- [9] Mayee F Chen, Daniel Y Fu, Dyah Adila, Michael Zhang, Frederic Sala, Kayvon Fatahalian, and Christopher Ré. Shoring up the foundations: Fusing model embeddings and weak supervision. In *Uncertainty in Artificial Intelligence*, pages 357–367. PMLR, 2022. 2
- [10] Richard J Chen, Tong Ding, Ming Y Lu, Drew FK Williamson, Guillaume Jaume, Andrew H Song, Bowen Chen, Andrew Zhang, Daniel Shao, Muhammad Shaban, et al. Towards a general-purpose foundation model for computational pathology. *Nature Medicine*, 30(3):850–862, 2024. 2
- [11] Zeming Chen, Alejandro Hernández Cano, Angelika Romanou, Antoine Bonnet, Kyle Matoba, Francesco Salvi, Matteo Pagliardini, Simin Fan, Andreas Köpf, Amirkeivan Mohtashami, et al. Meditron-70b: Scaling medical pretraining for large language models. *arXiv preprint arXiv:2311.16079*, 2023. 2
- [12] Zhihong Chen, Maya Varma, Jean-Benoit Delbrouck, Magdalini Paschali, Louis Blankemeier, Dave Van Veen, Jeya Maria Jose Valanarasu, Alaa Youssef, Joseph Paul Cohen, Eduardo Pontes Reis, et al. Chexagent: Towards a foundation model for chest x-ray interpretation. *arXiv preprint arXiv:2401.12208*, 2024. 2, 3, 6, 7, 8, 9
- [13] Eric W Christensen, Gregory N Nicola, Elizabeth Y Rula, Lauren P Nicola, Jennifer Hemingway, and Joshua A Hirsch. Budget neutrality and medicare physician fee schedule reimbursement trends for radiologists, 2005 to 2021. *Journal of the American College of Radiology*, 20(10):947–953, 2023. 1
- [14] Dina Demner-Fushman, Marc D Kohli, Marc B Rosenman, Sonya E Shooshan, Laritza Rodriguez, Sameer Antani, George R Thoma, and Clement J McDonald. Preparing a collection of radiology examinations for distribution and retrieval. *Journal of the American Medical Informatics Association*, 23(2):304–310, 2016. 2
- [15] Dina Demner-Fushman, Sophia Ananiadou, Makoto Miwa, Kirk Roberts, and Jun-ichi Tsujii. Bionlp workshop shared tasks. https://aclweb.org/aclwiki/BioNLP_Workshop#Shared_Tasks, 2024. Accessed: 2024-11-09. 2, 6
- [16] Ning Ding, Yujia Qin, Guang Yang, Fuchao Wei, Zonghan Yang, Yusheng Su, Shengding Hu, Yulin Chen, Chi-Min Chan, Weize Chen, et al. Parameter-efficient fine-tuning of large-scale pre-trained language models. *Nature Machine Intelligence*, 5(3):220–235, 2023. 2
- [17] Qingxiu Dong, Lei Li, Damai Dai, Ce Zheng, Jingyuan Ma, Rui Li, Heming Xia, Jingjing Xu, Zhiyong Wu, Tianyu Liu, et al. A survey on in-context learning. *arXiv preprint arXiv:2301.00234*, 2022. 2
- [18] Mark Endo, Rayan Krishnan, Viswesh Krishna, Andrew Y Ng, and Pranav Rajpurkar. Retrieval-based chest x-ray report generation using a pre-trained contrastive language-image model. In *Machine Learning for Health*, pages 209–219. PMLR, 2021. 2, 3, 6, 7, 9
- [19] Yunfan Gao, Yun Xiong, Xinyu Gao, Kangxiang Jia, Jinliu Pan, Yuxi Bi, Yi Dai, Jiawei Sun, Meng Wang, and Haofen Wang. Retrieval-augmented generation for large language models: A survey. *arXiv preprint arXiv:2312.10997*, 2023. 2
- [20] Ary L Goldberger, Luis AN Amaral, Leon Glass, Jeffrey M Hausdorff, Plamen Ch Ivanov, Roger G Mark, Joseph E Mietus, George B Moody, Chung-Kang Peng, and H Eugene Stanley. Physiobank, physiotoolkit, and physionet: components of a new research resource for complex physiologic signals. *circulation*, 101(23):e215–e220, 2000. 2
- [21] Yu Gu, Robert Tinn, Hao Cheng, Michael Lucas, Naoto Usuyama, Xiaodong Liu, Tristan Naumann, Jianfeng Gao, and Hoifung Poon. Domain-specific language model pre-training for biomedical natural language processing. *ACM Transactions on Computing for Healthcare (HEALTH)*, 3(1):1–23, 2021. 2, 8

- [22] Kaiming He, Xiangyu Zhang, Shaoqing Ren, and Jian Sun. Deep residual learning for image recognition. In *Proceedings of the IEEE conference on computer vision and pattern recognition*, pages 770–778, 2016. 4
- [23] Yuting He, Fuxiang Huang, Xinrui Jiang, Yuxiang Nie, Minghao Wang, Jiguang Wang, and Hao Chen. Foundation model for advancing healthcare: Challenges, opportunities, and future directions. *arXiv preprint arXiv:2404.03264*, 2024. 2
- [24] Ahmed Hosny, Chintan Parmar, John Quackenbush, Lawrence H Schwartz, and Hugo JWL Aerts. Artificial intelligence in radiology. *Nature Reviews Cancer*, 18(8):500–510, 2018. 1
- [25] Jeremy Irvin, Pranav Rajpurkar, Michael Ko, Yifan Yu, Silvana Ciurea-Ilcus, Chris Chute, Henrik Marklund, Behzad Haghgoo, Robyn Ball, Katie Shpanskaya, et al. Chexpert: A large chest radiograph dataset with uncertainty labels and expert comparison. In *Proceedings of the AAAI conference on artificial intelligence*, pages 590–597, 2019. 4, 5, 6, 8
- [26] Mohammed Ismail, Tarek N Hanna, Melissa A Davis, Eric Rubin, Ivan M DeQuesada, Randy C Miles, and Pari Pandharipande. The remote academic radiologist: Ajr expert panel narrative review. *American Journal of Roentgenology*, 222(5):e2329601, 2024. 1
- [27] Saahil Jain, Ashwin Agrawal, Adriel Saporta, Steven QH Truong, Du Nguyen Duong, Tan Bui, Pierre Chambon, Yuhao Zhang, Matthew P Lungren, Andrew Y Ng, et al. Radiograph: Extracting clinical entities and relations from radiology reports. *arXiv preprint arXiv:2106.14463*, 2021. 3, 6, 8
- [28] Jaehwan Jeong, Katherine Tian, Andrew Li, Sina Hartung, Subathra Adithan, Fardad Behzadi, Juan Calle, David Osayande, Michael Pohlen, and Pranav Rajpurkar. Multimodal image-text matching improves retrieval-based chest x-ray report generation. In *Medical Imaging with Deep Learning*, pages 978–990. PMLR, 2024. 2, 3, 6, 7, 9
- [29] Albert Q Jiang, Alexandre Sablayrolles, Arthur Mensch, Chris Bamford, Devendra Singh Chaplot, Diego de las Casas, Florian Bressand, Gianna Lengyel, Guillaume Lample, Lucile Saulnier, L elio Renard Lavaud, Marie-Anne Lachaux, Pierre Stock, Teven Le Scao, Thibaut Lavril, Thomas Wang, Timoth ee Lacroix, and William El Sayed. Mistral 7b. *arXiv preprint arXiv:2310.06825*, 2023. 8
- [30] Alistair Johnson, Lucas Bulgarelli, Tom Pollard, Leo A Celi, Roger Mark, and Steven Horng. Mimic-iv-ed (version 2.2). PhysioNet, 2023. <https://doi.org/10.13026/5ntk-km72>. 2
- [31] Alistair Johnson, Lucas Bulgarelli, Tom Pollard, Steven Horng, Leo A Celi, and Roger Mark. Mimic-iv (version 2.2). PhysioNet, 2023. <https://doi.org/10.13026/6mm1-ek67>. 2
- [32] Alistair Johnson, Matthew Lungren, Yifan Peng, Zhiyong Lu, Roger Mark, Seth Berkowitz, and Steven Horng. Mimic-cxr-jpg - chest radiographs with structured labels (version 2.1.0). PhysioNet, 2024. <https://doi.org/10.13026/jsn5-t979>. 4, 8
- [33] Alistair Johnson, Tom Pollard, Roger Mark, Seth Berkowitz, and Steven Horng. Mimic-cxr database (version 2.1.0). PhysioNet, 2024. <https://doi.org/10.13026/4jqj-jw95>. 4
- [34] Alistair EW Johnson, David J Stone, Leo A Celi, and Tom J Pollard. The mimic code repository: enabling reproducibility in critical care research. *Journal of the American Medical Informatics Association*, 25(1):32–39, 2018. 7, 2
- [35] Alistair EW Johnson, Tom J Pollard, Seth J Berkowitz, Nathaniel R Greenbaum, Matthew P Lungren, Chih-ying Deng, Roger G Mark, and Steven Horng. Mimic-cxr, a de-identified publicly available database of chest radiographs with free-text reports. *Scientific data*, 6(1):317, 2019. 2, 4, 7
- [36] Alistair EW Johnson, Tom J Pollard, Nathaniel R Greenbaum, Matthew P Lungren, Chih-ying Deng, Yifan Peng, Zhiyong Lu, Roger G Mark, Seth J Berkowitz, and Steven Horng. Mimic-cxr-jpg, a large publicly available database of labeled chest radiographs. *arXiv preprint arXiv:1901.07042*, 2019. 2, 4
- [37] Alistair EW Johnson, Lucas Bulgarelli, Lu Shen, Alvin Gayles, Ayad Shammout, Steven Horng, Tom J Pollard, Sicheng Hao, Benjamin Moody, Brian Gow, Li-wei H Lehman, Leo A Celi, and Roger Mark. Mimic-iv, a freely accessible electronic health record dataset. *Scientific data*, 10(1):1, 2023. 2
- [38] Brendan S Kelly, Conor Judge, Stephanie M Bollard, Simon M Clifford, Gerard M Healy, Awsam Aziz, Prateek Mathur, Shah Islam, Kristen W Yeom, Aonghus Lawlor, et al. Radiology artificial intelligence: a systematic review and evaluation of methods (raise). *European radiology*, 32(11):7998–8007, 2022. 1
- [39] Soryan Kumar, Aditya Khurana, Jack M Haglin, Douglas T Hidlay, Kevin Neville, Alan H Daniels, and Adam EM Eltorai. Trends in diagnostic imaging medicare reimbursements: 2007 to 2019. *Journal of the American College of Radiology*, 17(12):1584–1590, 2020. 1
- [40] Woosuk Kwon, Zhuohan Li, Siyuan Zhuang, Ying Sheng, Lianmin Zheng, Cody Hao Yu, Joseph E. Gonzalez, Hao Zhang, and Ion Stoica. Efficient memory management for large language model serving with pagedattention. In *Proceedings of the ACM SIGOPS 29th Symposium on Operating Systems Principles*, 2023. 5
- [41] Yanis Labrak, Adrien Bazoge, Emmanuel Morin, Pierre-Antoine Gourraud, Mickael Rouvier, and Richard Dufour. BioMistral: A collection of open-source pretrained large language models for medical domains. In *Findings of the Association for Computational Linguistics: ACL 2024*, pages 5848–5864. Association for Computational Linguistics, 2024. 8
- [42] Patrick Lewis, Ethan Perez, Aleksandra Piktus, Fabio Petroni, Vladimir Karpukhin, Naman Goyal, Heinrich K uttler, Mike Lewis, Wen-tau Yih, Tim Rockt aschel, et al. Retrieval-augmented generation for knowledge-intensive nlp tasks. *Advances in Neural Information Processing Systems*, 33:9459–9474, 2020. 2
- [43] Chin-Yew Lin. Rouge: A package for automatic evaluation of summaries. In *Text summarization branches out*, pages 74–81, 2004. 6

- [44] Hezheng Lin, Xing Cheng, Xiangyu Wu, and Dong Shen. Cat: Cross attention in vision transformer. In *2022 IEEE international conference on multimedia and expo (ICME)*, pages 1–6. IEEE, 2022. 3
- [45] Xi Victoria Lin, Akshat Shrivastava, Liang Luo, Srinivasan Iyer, Mike Lewis, Gargi Gosh, Luke Zettlemoyer, and Armen Aghajanyan. Moma: Efficient early-fusion pre-training with mixture of modality-aware experts. *arXiv preprint arXiv:2407.21770*, 2024. 2
- [46] Ming Y Lu, Bowen Chen, Drew FK Williamson, Richard J Chen, Ivy Liang, Tong Ding, Guillaume Jaume, Igor Odintsov, Long Phi Le, Georg Gerber, et al. A visual-language foundation model for computational pathology. *Nature Medicine*, 30(3):863–874, 2024. 2
- [47] Pablo Messina, Pablo Pino, Denis Parra, Alvaro Soto, Cecilia Besa, Sergio Uribe, Marcelo Andía, Cristian Tejos, Claudia Prieto, and Daniel Capurro. A survey on deep learning and explainability for automatic report generation from medical images. *ACM Computing Surveys (CSUR)*, 54(10s):1–40, 2022. 1, 2
- [48] Meta. Llama 3.2: Revolutionizing edge ai and vision with open, customizable models. <https://ai.meta.com/blog/llama-3-2-connect-2024-vision-edge-mobile-devices/>, 2024. Accessed: 2024-11-08. 2
- [49] Sewon Min, Xinxu Lyu, Ari Holtzman, Mikel Artetxe, Mike Lewis, Hannaneh Hajishirzi, and Luke Zettlemoyer. Rethinking the role of demonstrations: What makes in-context learning work? *arXiv preprint arXiv:2202.12837*, 2022. 2
- [50] MistralAI. Mistral 7b instruct v0.3. <https://huggingface.co/mistralai/Mistral-7B-Instruct-v0.3>, 2024. Accessed: 2024-11-11. 5, 8
- [51] Michael Moor, Oishi Banerjee, Zahra Shakeri Hossein Abad, Harlan M Krumholz, Jure Leskovec, Eric J Topol, and Pranav Rajpurkar. Foundation models for generalist medical artificial intelligence. *Nature*, 616(7956):259–265, 2023. 2
- [52] Reabal Najjar. Redefining radiology: a review of artificial intelligence integration in medical imaging. *Diagnostics*, 13(17):2760, 2023. 1
- [53] Peter Neidlinger, Omar SM El Nahhas, Hannah Sophie Muti, Tim Lenz, Michael Hoffmeister, Hermann Brenner, Marko van Treeck, Rupert Langer, Bastian Dislich, Hans Michael Behrens, et al. Benchmarking foundation models as feature extractors for weakly-supervised computational pathology. *arXiv preprint arXiv:2408.15823*, 2024. 2
- [54] Dang Nguyen, Chacha Chen, He He, and Chenhao Tan. Pragmatic radiology report generation. In *Machine Learning for Health (ML4H)*, pages 385–402. PMLR, 2023. 2, 3, 4, 7
- [55] Ha Q Nguyen, Khanh Lam, Linh T Le, Hieu H Pham, Dat Q Tran, Dung B Nguyen, Dung D Le, Chi M Pham, Hang TT Tong, Diep H Dinh, et al. Vindr-cxr: An open dataset of chest x-rays with radiologist’s annotations. *Scientific Data*, 9(1):429, 2022. 2
- [56] Aaron Nicolson, Jason Dowling, Douglas Anderson, and Bevan Koopman. Longitudinal data and a semantic similarity reward for chest x-ray report generation. *Informatics in Medicine Unlocked*, 50:101585, 2024. 2, 3, 6
- [57] Aaron Nicolson, Jinghui Liu, Jason Dowling, Anthony Nguyen, and Bevan Koopman. e-health csiro at rrg24: Entropy-augmented self-critical sequence training for radiology report generation. *arXiv preprint arXiv:2408.03500*, 2024. 6, 7, 8, 9
- [58] Harsha Nori, Yin Tat Lee, Sheng Zhang, Dean Carignan, Richard Edgar, Nicolo Fusi, Nicholas King, Jonathan Larson, Yuanzhi Li, Weishung Liu, et al. Can generalist foundation models outcompete special-purpose tuning? case study in medicine. *arXiv preprint arXiv:2311.16452*, 2023. 2
- [59] European Society of Radiology (ESR). Good practice for radiological reporting. guidelines from the european society of radiology (esr). *Insights into imaging*, 2(2):93–96, 2011. 2
- [60] Kishore Papineni, Salim Roukos, Todd Ward, and Wei-Jing Zhu. Bleu: a method for automatic evaluation of machine translation. In *Proceedings of the 40th annual meeting of the Association for Computational Linguistics*, pages 311–318, 2002. 6
- [61] F. Pedregosa, G. Varoquaux, A. Gramfort, V. Michel, B. Thirion, O. Grisel, M. Blondel, P. Prettenhofer, R. Weiss, V. Dubourg, J. Vanderplas, A. Passos, D. Cournapeau, M. Brucher, M. Perrot, and E. Duchesnay. Scikit-learn: Machine learning in Python. *Journal of Machine Learning Research*, 12:2825–2830, 2011. 2
- [62] Alec Radford, Jong Wook Kim, Chris Hallacy, Aditya Ramesh, Gabriel Goh, Sandhini Agarwal, Girish Sastry, Amanda Askell, Pamela Mishkin, Jack Clark, et al. Learning transferable visual models from natural language supervision. In *International conference on machine learning*, pages 8748–8763. PMLR, 2021. 3
- [63] Vignav Ramesh, Nathan Chi, and Pranav Rajpurkar. Cxrpro: Mimic-cxr with prior references omitted (version 1.0.0). PhysioNet, 2022. <https://doi.org/10.13026/frag-yn96>. 3
- [64] Vignav Ramesh, Nathan A Chi, and Pranav Rajpurkar. Improving radiology report generation systems by removing hallucinated references to non-existent priors. In *Machine Learning for Health*, pages 456–473. PMLR, 2022. 2, 3, 6, 7, 9
- [65] Mercy Ranjit, Gopinath Ganapathy, Ranjit Manuel, and Tanuja Ganu. Retrieval augmented chest x-ray report generation using openai gpt models. In *Machine Learning for Healthcare Conference*, pages 650–666. PMLR, 2023. 2, 3, 7
- [66] Abi Rimmer. Radiologist shortage leaves patient care at risk, warns royal college. *BMJ: British Medical Journal (Online)*, 359, 2017. 1
- [67] Andrew B Rosenkrantz, Danny R Hughes, and Richard Duszak Jr. Increasing subspecialization of the national radiologist workforce. *Journal of the American College of Radiology*, 17(6):812–818, 2020. 1
- [68] Khaled Saab, Tao Tu, Wei-Hung Weng, Ryutaro Tanno, David Stutz, Ellery Wulczyn, Fan Zhang, Tim Strother, Chunjong Park, Elahe Vedadi, et al. Capabilities of gem-

- ini models in medicine. *arXiv preprint arXiv:2404.18416*, 2024. 2
- [69] Phillip Sloan, Philip Clatworthy, Edwin Simpson, and Majid Mirmehdi. Automated radiology report generation: A review of recent advances. *IEEE Reviews in Biomedical Engineering*, 2024. 1, 2
- [70] Akshay Smit, Saahil Jain, Pranav Rajpurkar, Anuj Pareek, Andrew Y Ng, and Matthew P Lungren. Chexbert: combining automatic labelers and expert annotations for accurate radiology report labeling using bert. *arXiv preprint arXiv:2004.09167*, 2020. 3, 6, 8
- [71] Matteo Stefanini, Marcella Cornia, Lorenzo Baraldi, Silvia Cascianelli, Giuseppe Fiameni, and Rita Cucchiara. From show to tell: A survey on deep learning-based image captioning. *IEEE transactions on pattern analysis and machine intelligence*, 45(1):539–559, 2022. 2
- [72] Liwen Sun, James Zhao, Megan Han, and Chenyan Xiong. Fact-aware multimodal retrieval augmentation for accurate medical radiology report generation. *arXiv preprint arXiv:2407.15268*, 2024. 2, 3, 7
- [73] Tim Tanida, Philip Müller, Georgios Kaissis, and Daniel Rueckert. Interactive and explainable region-guided radiology report generation. In *Proceedings of the IEEE/CVF Conference on Computer Vision and Pattern Recognition*, pages 7433–7442, 2023. 2, 3, 6, 7, 9
- [74] Anja Thieme, Aditya Nori, Marzyeh Ghassemi, Rishi Bommasani, Tariq Osman Andersen, and Ewa Luger. Foundation models in healthcare: opportunities, risks & strategies forward. In *Extended Abstracts of the 2023 CHI Conference on Human Factors in Computing Systems*, pages 1–4, 2023. 2
- [75] Lukas Tuggener, Pascal Sager, Yassine Taoudi-Benchekroun, Benjamin F Grewe, and Thilo Stadelmann. So you want your private llm at home?: a survey and benchmark of methods for efficient gpts. In *11th IEEE Swiss Conference on Data Science (SDS), Zurich, Switzerland, 30-31 May 2024*. ZHAW Zürcher Hochschule für Angewandte Wissenschaften, 2024. 2
- [76] Ashish Vaswani, Noam Shazeer, Niki Parmar, Jakob Uszkoreit, Llion Jones, Aidan N Gomez, Łukasz Kaiser, and Illia Polosukhin. Attention is all you need. In *Advances in Neural Information Processing Systems*. Curran Associates, Inc., 2017. 3
- [77] Maria De La Iglesia Vayá, Jose Manuel Saborit, Joaquim Angel Montell, Antonio Pertusa, Aurelia Bustos, Miguel Cazorla, Joaquin Galant, Xavier Barber, Domingo Orozco-Beltrán, Francisco García-García, et al. Bimcv covid-19+: a large annotated dataset of rx and ct images from covid-19 patients. *arXiv preprint arXiv:2006.01174*, 2020. 2
- [78] Michael Wornow, Yizhe Xu, Rahul Thapa, Birju Patel, Ethan Steinberg, Scott Fleming, Michael A Pfeffer, Jason Fries, and Nigam H Shah. The shaky foundations of large language models and foundation models for electronic health records. *npj Digital Medicine*, 6(1):135, 2023. 2
- [79] Feiyang Yu, Mark Endo, Rayan Krishnan, Ian Pan, Andy Tsai, Eduardo Pontes Reis, Eduardo Kaiser Ururahy Nunes Fonseca, Henrique Min Ho Lee, Zahra Shakeri Hossein Abad, Andrew Y Ng, et al. Evaluating progress in automatic chest x-ray radiology report generation. *Patterns*, 4(9), 2023. 8
- [80] Shaoting Zhang and Dimitris Metaxas. On the challenges and perspectives of foundation models for medical image analysis. *Medical image analysis*, 91:102996, 2024. 2
- [81] Sheng Zhang, Yanbo Xu, Naoto Usuyama, Hanwen Xu, Jaspreet Bagga, Robert Tinn, Sam Preston, Rajesh Rao, Mu Wei, Naveen Valluri, et al. Biomedclip: a multimodal biomedical foundation model pretrained from fifteen million scientific image-text pairs. *arXiv preprint arXiv:2303.00915*, 2023. 2
- [82] Tianyi Zhang*, Varsha Kishore*, Felix Wu*, Kilian Q. Weinberger, and Yoav Artzi. Bertscore: Evaluating text generation with bert. In *International Conference on Learning Representations*, 2020. 6

LaB-RAG: Label Boosted Retrieval Augmented Generation for Radiology Report Generation

Supplementary Material

S1. Abbreviations and Terms

Term	Meaning
LaB-RAG	Label Boosted Retrieval Augmented Generation
Label Filtering	Using categorical labels to filter retrieved examples
Label Formatting	Using categorical labels as text descriptors of images
RRG	Radiology report generation
CXR	Chest X-ray
AP	Anterior-posterior (<i>i.e.</i> from front to back)
PICC	Peripherally inserted central catheter
SVC	Superior vena cava
AI	Artificial intelligence
ML	Machine learning
DL	Deep learning
LLM	Large language model
RAG	Retrieval augmented generation
FM	Foundation model
SFT	Supervised fine-tuning
PEFT	Parameter-efficient fine-tuning
ICL	In-context learning
SOTA	State of the art
NLP	Natural language processing
CLIP	Contrastive language-image pretraining

Table S1. Reference of abbreviations.

S2. Dataset Extended Information

MIMIC-CXR [35] imaging studies were collected in the emergency department at the Beth Israel Deaconess Medical Center (BIDMC) in Boston, MA between 2011 and 2016. Multiple chest X-rays may be present for a single study, and a patient may have multiple imaging studies. The training, validation, and testing splits provided by MIMIC-CXR are split at the patient level, meaning all images for all studies belonging to a single patient are contained in one split. The demographic breakdown of studies in each split is presented in Tab. S2, though the final number of patients and imaging studies considered in each of our experiments depends on the availability of all required data modalities. Demographic information was collected from the MIMIC-IV v2.2 [31, 37] *hosp* module and MIMIC-IV-ED v2.2 [30]. All data were accessed through PhysioNet [20].

For images, we select one image per study by preferentially selecting images based on the captured view position. The number of selected image views per split is listed in Tab. S3. We follow the order of preference for view positions from the ACL 2024 BioNLP workshop’s RRG shared task [15]; the exact list can be found in Tab. S4. We use code inspired by the MIMIC Code Repository [34] to extract radiology report sections from the free text reports. The number of extracted findings and impression sections per split is listed in Tab. S5.

Ethical Considerations for Data Usage. As the MIMIC [37] datasets were collected from the BIDMC, the BIDMC institutional review board (IRB) granted a waiver of informed consent and approved the collection and sharing of the data for research purposes following proper de-identification according to HIPAA. As users of the data, we follow procedures outlined by PhysioNet [20] to have all researchers with data access complete human research training and sign a data use agreement (DUA). We strictly control access to the data in our compute environments and make no efforts to re-identify data subjects from any free-text data (which may have escaped de-identification) or any other sources. Additionally, as we do no fine-tuning of our own LLMs, we do not need to consider whether it is a DUA violation to share LLM weights which may have memorized and can reproduce training text.

S3. LaB-Classifier Training Details

We fit 14 per-label binary logistic regressions over the unprojected 512d image embeddings from BioViL-T (see Sec. 3.2). We derive ground-truth labels to train our models with by binarizing the CheXpert labels as positive (value of 1) or not (value of 0, -1, or null). We fit the models on the training split and find a per-label probability threshold which maximizes the f1-score over the validation split. The receiver operator characteristic and precision recall curves

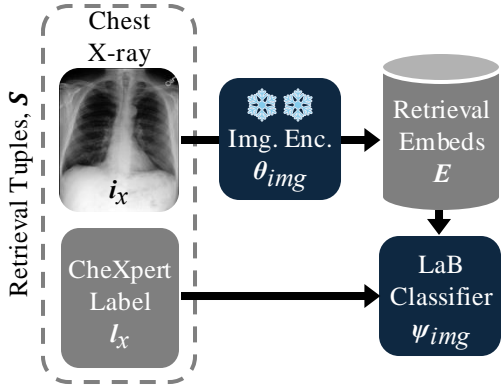


Figure S1. Overview of training per-label LaB-Classifier logistic regressions.

of the 14 labels over the test split are presented in Fig. S2. We adopt the same heuristic as above for computing the “Other” label for the image. For training the logistic classifiers, we use `sklearn` [61] v1.5.1 with L2 regularization, the `saga` solver for 500 iterations, and otherwise default hyperparameters.

S4. Evaluation Strategy Extended Details

For all metrics, actual and generated text are input as whole reports; reports are not split on the sentence level. This gives a score between 0 and 1 for each report for each metric. We compare results by considering the per-metric scores across all reports. We show barplots of the per-metric average scores with errorbars showing the standard error. To test for statistical significance, we perform paired t-tests within one set of experiments, applying Bonferroni correction for the number of comparisons made within a single metric. For experiments on variations of LaB-RAG, we compare all pairwise combinations of the variants; for comparing to literature models, we only consider pairs including LaB-RAG. Statistically significant pairs are annotated with brackets in the barplot with “*” denoting $p < 0.05$; non-significant pairs are not annotated. We refer to our code for precise implementation details.

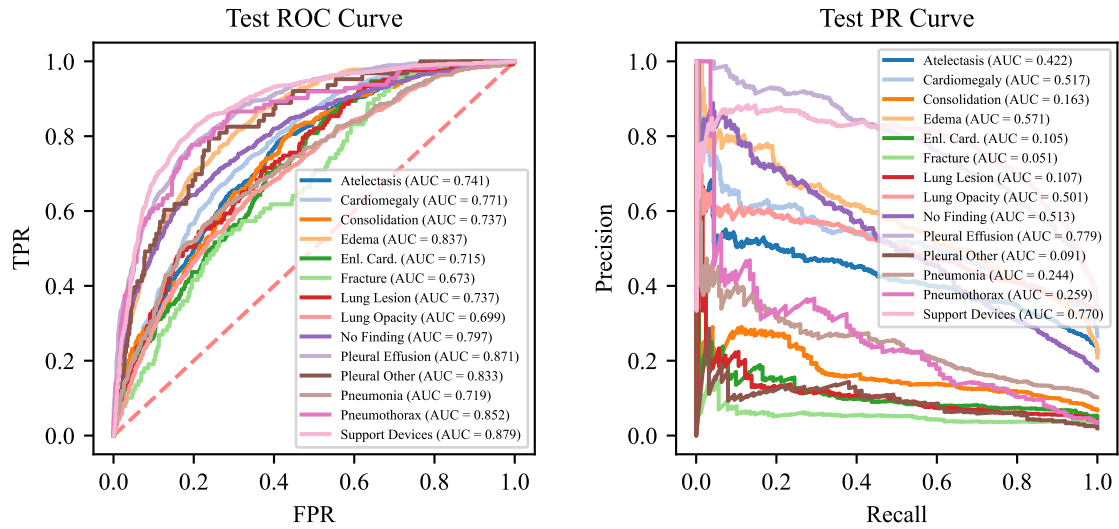


Figure S2. Test set ROC and PR curves of LaB-Classifier, a set of 14 per-label logistic regressions.

		Overall	Train	Val	Test
Count, N	Patients	65379	64586	500	293
	Studies	227835	222758	1808	3269
Age	Median [Q1,Q3]	65 [52,76]	65 [52,76]	63 [52,77]	69 [61,77]
	Missing, N (%)	11825 (5.2)	11522 (5.2)	134 (7.4)	169 (5.2)
Sex, N (%)	Female	105117 (48.7)	102951 (48.7)	737 (44.0)	1429 (46.1)
	Male	110893 (51.3)	108285 (51.3)	937 (56.0)	1671 (53.9)
	Missing	11825 (5.2)	11522 (5.2)	134 (7.4)	169 (5.2)
Race, N (%)	White	141531 (65.5)	138343 (65.5)	1081 (64.6)	2107 (68.0)
	Black	35788 (16.6)	34920 (16.5)	186 (11.1)	682 (22.0)
	Hispanic or Latino	12358 (5.7)	12150 (5.8)	110 (6.6)	98 (3.2)
	Other	9088 (4.2)	8857 (4.2)	190 (11.4)	41 (1.3)
	Unknown	8430 (3.9)	8343 (4.0)	51 (3.0)	36 (1.2)
	Asian	7927 (3.7)	7753 (3.7)	47 (2.8)	127 (4.1)
	AIAN	644 (0.3)	628 (0.3)	7 (0.4)	9 (0.3)
	NHPI	205 (0.1)	203 (0.1)	2 (0.1)	0 (0.0)
	Missing	11864 (5.2)	11561 (5.2)	134 (7.4)	169 (5.2)

Table S2. Per-study demographic breakdown of MIMIC defined training/validation/testing splits. AIAN = American Indian or Alaska Native, NHPI = Native Hawaiian or Pacific Islander.

View, N (%)	Overall	Train	Val	Test
PA	85867 (37.7)	84323 (37.9)	661 (36.6)	883 (27.0)
AP	132264 (58.1)	129034 (57.9)	1072 (59.3)	2158 (66.0)
LATERAL	176 (0.1)	172 (0.1)	2 (0.1)	2 (0.1)
LL	2225 (1.0)	2160 (1.0)	17 (0.9)	48 (1.5)
AP AXIAL	1 (0.0)	1 (0.0)	0 (0.0)	0 (0.0)
LAO	1 (0.0)	1 (0.0)	0 (0.0)	0 (0.0)
LPO	1 (0.0)	1 (0.0)	0 (0.0)	0 (0.0)

Table S3. Count of selected single view per-study. PA = postero-anterior, AP = antero-posterior, LL = left lateral, LAO = left anterior oblique, LPO = left posterior oblique.

Rank	View	Rank	View	Rank	View
1	PA	6	AP LLD	11	RAO
2	AP	7	AP RLD	12	LPO
3	LATERAL	8	PA RLD	13	XTABLE LATERAL
4	LL	9	PA LLD	14	SWIMMERS
5	AP AXIAL	10	LAO	15	(Empty String)

Table S4. Order of view preference for selecting single image for multi-image studies. PA = postero-anterior, AP = antero-posterior, LL = left lateral, LLD = left lateral decubitus, RLD = right lateral decubitus, LAO = left anterior oblique, RAO = , LPO = left posterior oblique.

Section, N (%)	Overall	Train	Val	Test
Impression	189561 (83.2)	185816 (83.4)	1521 (84.1)	2224 (68.0)
Findings	155716 (68.3)	152173 (68.3)	1196 (66.2)	2347 (71.8)
Both	128032 (56.2)	125417 (56.3)	991 (54.8)	1624 (49.7)

Table S5. Count of reports with extracted “Findings”, “Impression”, or both sections.

S5. Prompts

Prompt Type	Prompt Text
Naive	<p>You are an expert radiological assistant. Your task is to generate a radiology report after <<Report>> given context information. The context information contains examples of reports written for similar cases. Use the examples to generate a report for the current case. Strictly follow the instructions below to generate the reports.</p> <p>**Instructions**</p> <ol style="list-style-type: none">1. The report must be based on the information in the context.2. The report must mimic the style of the reports shown in the context.3. Do not generate blank reports. <p>CONTEXT: Example: 1 <i>(Report Text)</i></p> <p><i>(More Examples)</i></p> <p>Now generate the report for the current case. Always generate reports based on the examples shown. <<Report>></p>

Table S6. The “Naive” prompt does not incorporate labels.

Prompt Type	Prompt Text
Simple	<p>You are an expert radiological assistant. Your task is to generate a radiology report after <<Report>> given context information. The context information contains examples of reports written for similar cases and their associated labels. Use the examples and their associated labels to generate a report for the current case based on the current label. Strictly follow the instructions below to generate the reports.</p> <p>**Instructions**</p> <ol style="list-style-type: none"> 1. The report must be based on the information in the context and the current label. 2. The report must mimic the style of the reports shown in the context. 3. Do not generate blank reports. <p>CONTEXT: Example: 1 Label: <i>(Positive Labels)</i> <i>(Report Text)</i></p> <p><i>(More Examples)</i></p> <p>Now generate the report for the current case using its label below. Always generate reports based on the examples shown. Label: <i>(Positive Labels)</i> <<Report>></p>

Table S7. The “Simple” prompt formats positive labels for the examples and target image.

Prompt Type	Prompt Text
Verbose	<p>You are an expert radiological assistant. Your task is to generate a radiology report after <<Report>> given context information. The context information contains examples of reports written for similar cases and their associated labels. The labels provided are expert annotations. More information about the labels is described below.</p> <p>The individual labels used represent common chest radiographic observations and fall under four categories: ‘Positive’, ‘Negative’, ‘Uncertain’ and ‘Unmentioned’. These categories correspond to the mention or presence of the labels or their equivalent in the report. Below is a description and example of each of the label categories:</p> <ol style="list-style-type: none"> 1. ‘Positive’: A label is positive if the associated observation or disease is stated as present in the report, for example: ‘moderate bilateral effusions observed’. 2. ‘Negative’: A label is negative if the associated observation or disease is stated as absent in the report, for example: ‘no evidence of pulmonary edema’. 3. ‘Uncertain’: A label is uncertain if there is ambiguity about the presence or absence of the associated observation or disease in the report, for example: ‘pneumonia cannot be excluded in the appropriate clinical context’. 4. ‘Unmentioned’: A label is unmentioned if there is no mention of the associated observation or disease in report. <p>Use the examples, their associated labels, and the label descriptions to generate a report for the current case based on the current label. Strictly follow the instructions below to generate the reports.</p> <p>**Instructions**</p> <ol style="list-style-type: none"> 1. The report must be based on the information in the context and the current label. 2. The report must mimic the style of the reports shown in the context. 3. Do not generate blank reports. <p>CONTEXT: Example: 1 Positive: <i>(Positive Labels)</i> Negative: <i>(Negative Labels)</i> Uncertain: <i>(Uncertain Labels)</i> Unmentioned: <i>(Unmentioned Labels)</i> <i>(Report Text)</i></p> <p><i>(More Examples)</i></p> <p>Now generate the report for the current case using its label below. Always generate reports based on the examples shown. Positive: <i>(Positive Labels)</i> Negative: <i>(Negative Labels)</i> Uncertain: <i>(Uncertain Labels)</i> Unmentioned: <i>(Unmentioned Labels)</i> <<Report>></p>

Table S8. The “Verbose” prompt formats positive, negative, uncertain, and unmentioned labels for the examples and target image.

Prompt Type	Prompt Text
	<i>(Same as Verbose)</i>
	Instructions
Instruct	<ol style="list-style-type: none"> 1. The report must be based on the information in the context and the current label. 2. The report must mimic the style of the reports shown in the context. 3. Do not generate blank reports. 4. Ensure that the positive labels are clearly described as being present in the report, using example language from the context. 5. Ensure that the negative labels are clearly described as being absent in the report, using example language from the context. 6. Describe the uncertain labels as necessary. 7. Ensure that the unmentioned labels are not mentioned in the report.
	<i>(Same as Verbose)</i>

Table S9. The “Instruct” prompt uses the same label format as “Verbose” and adds additional instructions.

S6. Literature Model Inference

In this section, we provide our extended descriptions for baseline models from the literature. We select models based on model architecture, generated report section, SOTA performance on evaluation metrics, and finally availability of open source inference code. The final set of models we compare against are as follows: CXR-RePaiR [18], CXR-ReDonE [64], X-REM [28], RGRG [73], CheXagent [12], and CXRMate-RRG24 [57]. We compare models over the intersection of each method’s test split subsets.

CXR-RePaiR formulates report generation as a pure retrieval task. It uses a model, trained via CLIP on radiology report-image pairs from MIMIC-CXR, to rank similarity between test images and a large retrieval corpus. We use the mode of CXR-RePaiR where the generated report output is the the top-1 retrieved whole reports.

CXR-RePaiR generates the “Impression” section over the MIMIC-CXR test split. Only the subset of the test split with an extractable “Impression” section is considered. While we adopt a similar strategy, CXR-RePaiR uses a custom implementation of “Impression” section extraction that differs from ours. CXR-RePaiR thus uses 2192 test studies as compared to our “Impression” test split of 2224.

CXR-ReDonE improves upon CXR-RePaiR by preprocessing the training and retrieval reports to remove references to prior imaging studies. Additionally, the joint-embedding model was trained via ALBEF instead of CLIP. We use the provided checkpoint of the retrieval model which was trained over the new data and via the new method; we do inference using whole reports with priors omitted as the retrieval set. The generated reports are then the top-1 retrieved whole report. CXR-ReDonE uses the “Impression” sections preprocessed by CXR-RePaiR and so results in the same test split subset.

X-REM also trains a vision-language model via ALBEF, however they introduce a novel similarity metric during training which incorporates CheXbert labels. An intermediary step retrieves the top-10 whole reports ranked by their new similarity score. Finally, they apply a model-based natural language filter to each retrieved report and only select those that are deemed relevant up to a limit; we adopt the author default limit of 2 reports, thus the output report is a concatenation of up to 2 reports. X-REM also uses the “Impression” sections preprocessed by CXR-RePaiR with the same test split subset.

CheXagent is presented by its authors as a foundation model trained to follow instructions in the CXR domain. CheXagent follows a complex training scheme and utilizes other CXR datasets. At a high-level, CheXagent is trained by aligning image latent embeddings to the an LLM’s token embedding space. Additionally, the authors introduce a novel dataset for instruction tuning, their final training step.

CheXagent is able to generate both “Findings” and “Impression” sections. “Impression” generated is simply prompted with “Generate impression”. “Findings” are generated by concatenating generations of individual “Local Findings” per anatomical compartment. “Local Findings” are generated by prompting with “Describe [Anatomical Compartment]” where the compartments are: “Airway”, “Breathing”, “Cardiac”, “Diaphragm” and “Everything else (e.g., mediastinal contours, bones, soft tissues, tubes, valves, and pacemakers)”. These compartments were inspired by documentation provided by the authors. CheXagent inference code is flexible and allows for generation over our specified subsets of the test split for “Findings”, “Impression”, or both sections.

CXRMate uses an encoder-decoder transformer architecture. It is both able to generate a single report over multiple images from a single imaging study and it takes as input reports from prior studies. Additionally, it is trained with a complex reinforcement learning framework. Interestingly, the authors experiment with RadGraph and CXR-BERT in their reward function, arguing that CXR-BERT better captures radiology report semantics; CXR-BERT is the language encoder of the vision-language model BioViL [4].

We specifically use the checkpoint of CXRMate submitted to the ACL 2024 BioNLP workshop’s task for RRG [57], though we only input the single image per study defined by our data preprocessing steps. While CheXagent generates both “Findings” and “Impression” jointly, the model provides a utility to split these sections after generation. We are then able to run inference using our subsets of the test split for which we have “Findings”, “Impression”, or both sections.

RGRG generates the “Findings” section of a report by combining individual sentences that describe specific anatomical regions. This is accomplished by training a model over a specialized dataset, derived from MIMIC-CXR, which pairs anatomical region bounding boxes with sentences from the corresponding report detailing those regions. Thus RGRG learns to extract localized image latent embeddings to generate sentences grounded in the specific anatomical feature. As RGRG’s language model is a decoder-only transformer, the image embeddings are prepended input as tokens. Unlike CheXagent, where individual anatomical regions must be prompted by the user, RGRG automatically selects relevant regions using a custom trained object detector model. As RGRG only generates the “Findings”, we evaluate using our test split subset for studies with an extractable “Findings” section.

S7. Supplemental Results

Experiment	Section	Variable	bleu4	rougeL	bertscore	f1radgraph	f1chexbert		
Baselines	Findings	LaB-RAG	0.042	0.204	0.861	0.183	0.466		
		RGRG	0.071	0.210	0.860	0.215	0.435		
		CheXagent	0.061	0.232	0.861	0.234	0.412		
		CXRMate	0.064	0.229	0.861	0.247	0.469		
	Impression	LaB-RAG	0.042	0.204	0.861	0.183	0.466		
		CXR-RePaiR	0.020	0.124	0.848	0.108	0.347		
		CXR-ReDonE	0.009	0.130	0.845	0.103	0.333		
		X-REM	0.013	0.162	0.854	0.139	0.408		
		CheXagent	0.060	0.209	0.864	0.176	0.397		
		CXRMate	0.053	0.212	0.862	0.191	0.422		
	Both	LaB-RAG	0.042	0.204	0.861	0.183	0.466		
		CheXagent	0.093	0.263	0.870	0.272	0.415		
CXRMate		0.087	0.253	0.866	0.271	0.438			
Filter & Format	Findings	Standard RAG	0.043	0.201	0.858	0.183	0.409		
		Label Filter only	0.041	0.198	0.857	0.180	0.443		
		Label Format only	0.045	0.208	0.863	0.193	0.466		
		LaB-RAG	0.042	0.204	0.861	0.183	0.466		
	Impression	Standard RAG	0.020	0.149	0.851	0.137	0.382		
		Label Filter only	0.023	0.152	0.851	0.144	0.438		
		Label Format only	0.033	0.172	0.858	0.152	0.446		
		LaB-RAG	0.032	0.168	0.856	0.146	0.450		
Filter	Findings	No-filter	0.045	0.208	0.863	0.193	0.466		
		Exact	0.042	0.204	0.861	0.183	0.466		
		Partial	0.043	0.205	0.862	0.185	0.467		
	Impression	No-filter	0.033	0.172	0.858	0.152	0.446		
		Exact	0.032	0.168	0.856	0.146	0.450		
		Partial	0.033	0.174	0.858	0.154	0.451		
Format	Findings	Naive	0.041	0.198	0.857	0.180	0.443		
		Simple	0.042	0.204	0.861	0.183	0.466		
		Verbose	0.040	0.196	0.856	0.180	0.438		
		Instruct	0.039	0.195	0.855	0.180	0.433		
	Impression	Naive	0.023	0.152	0.851	0.144	0.438		
		Simple	0.032	0.168	0.856	0.146	0.450		
		Verbose	0.013	0.147	0.847	0.134	0.400		
		Instruct	0.013	0.146	0.846	0.131	0.393		
		LLM	Findings	Mistral-v1	0.037	0.178	0.850	0.181	0.454
				BioMistral	0.038	0.197	0.857	0.168	0.445
Mistral-v3	0.042			0.204	0.861	0.183	0.466		
Impression	Mistral-v1		0.017	0.124	0.838	0.139	0.446		
	BioMistral		0.029	0.160	0.851	0.131	0.402		
	Mistral-v3		0.032	0.168	0.856	0.146	0.450		
Label	Findings	True	0.055	0.221	0.866	0.203	0.568		
		Predicted	0.042	0.204	0.861	0.183	0.466		
	Impression	True	0.047	0.229	0.871	0.221	0.800		
		Predicted	0.032	0.168	0.856	0.146	0.450		
Section	Intersection	Findings-Intersect	0.050	0.214	0.863	0.197	0.431		
		Impression-Intersect	0.039	0.182	0.860	0.151	0.430		
		Both	0.061	0.226	0.865	0.211	0.456		

Table S10. Full experimental results. By default, LaB-RAG uses “Exact” filter, “Simple” format/prompt, Mistral-v3, and predicted labels.

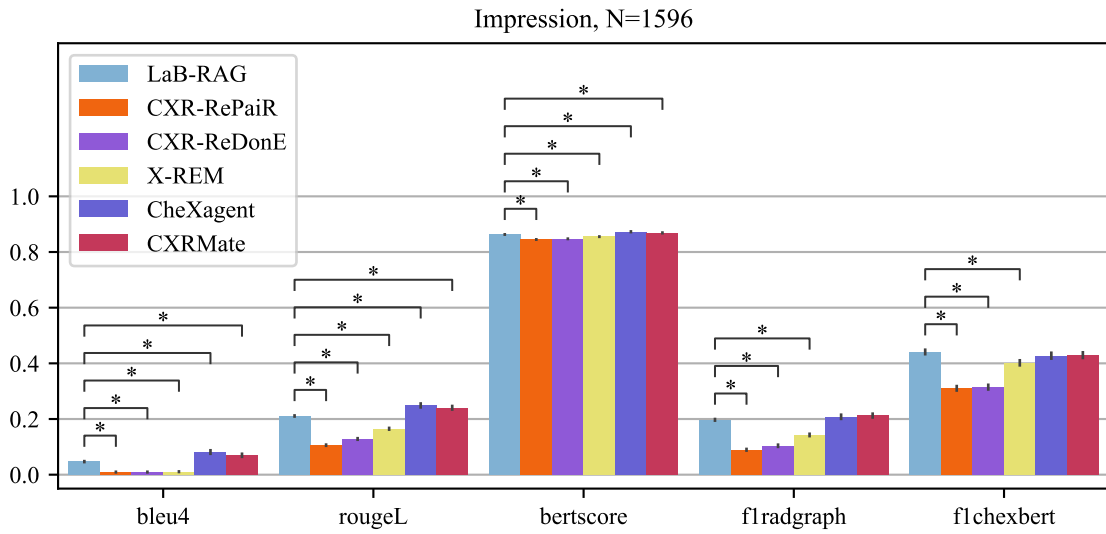
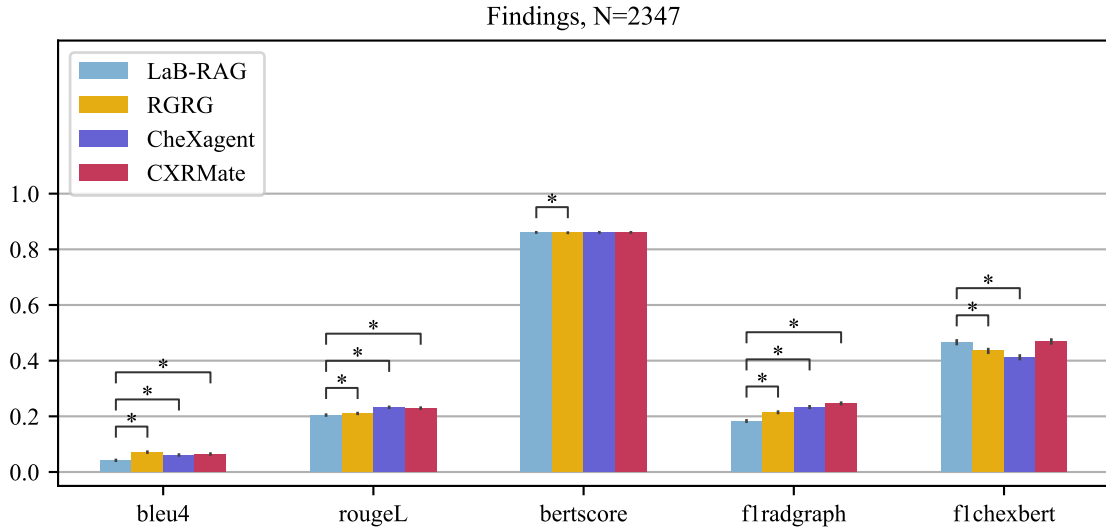


Figure S3. Comparison of LaB-RAG to literature baselines. Significantly different pairs by paired t-test annotated if $p < 0.05$, Bonferroni correction applied for number of comparisons vs LaB-RAG. By default, LaB-RAG uses “Exact” filter, “Simple” format/prompt, Mistral-v3, and predicted labels.

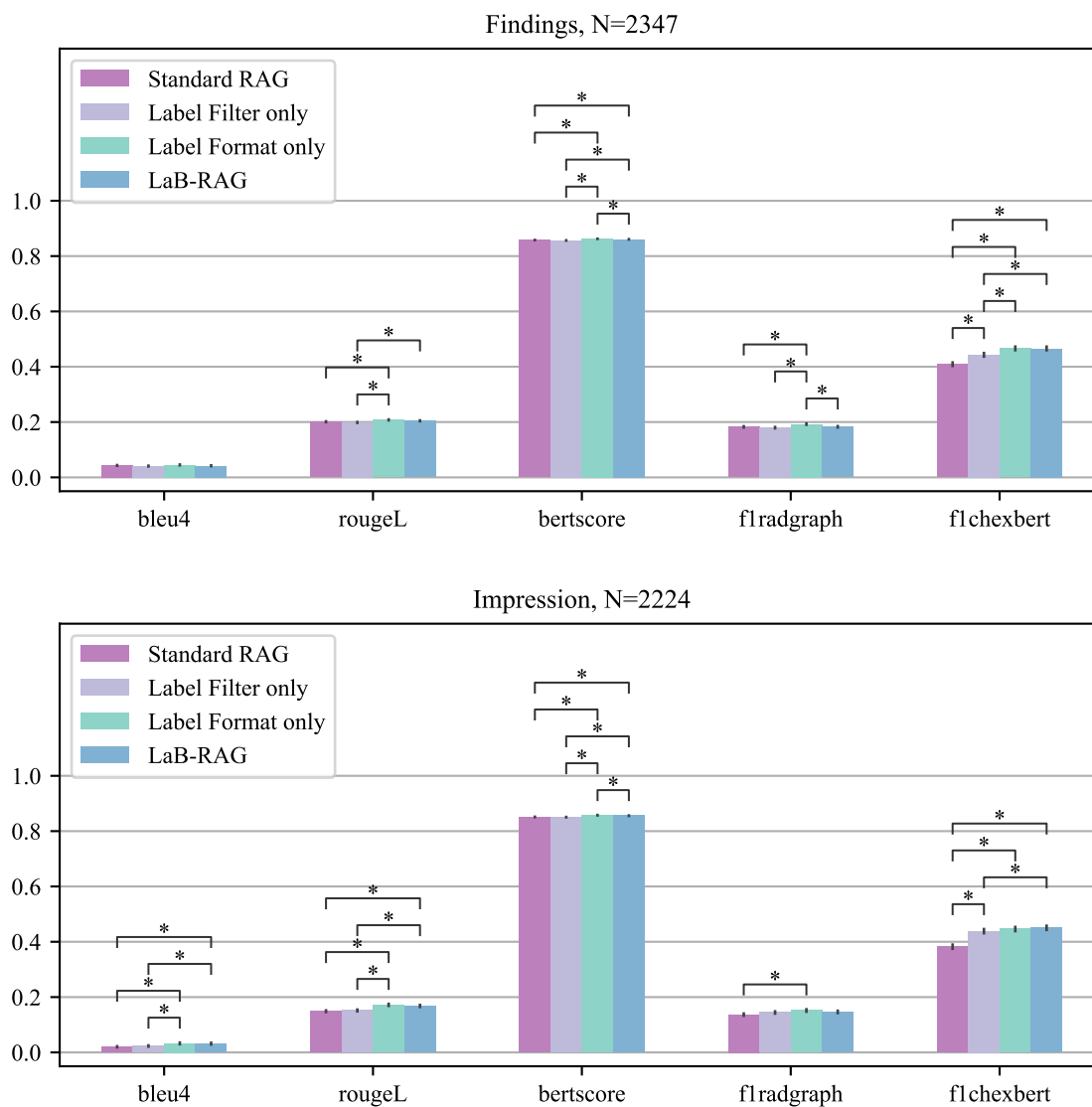


Figure S4. Comparison of label filter and format components of LaB-RAG. Significantly different pairs by paired t-test annotated if $p < 0.05$, Bonferroni correction applied for number of all pairwise comparisons per-plot. “Standard RAG” uses “No-filter” filter and “Naive” format/prompt. “Label Filter only” uses “Exact” filter and “Naive” format/prompt. “Label Format only” uses “No-filter” filter and “Simple” format/prompt. LaB-RAG otherwise defaults to “Exact” filter, “Simple” format/prompt, Mistral-v3, and predicted labels.

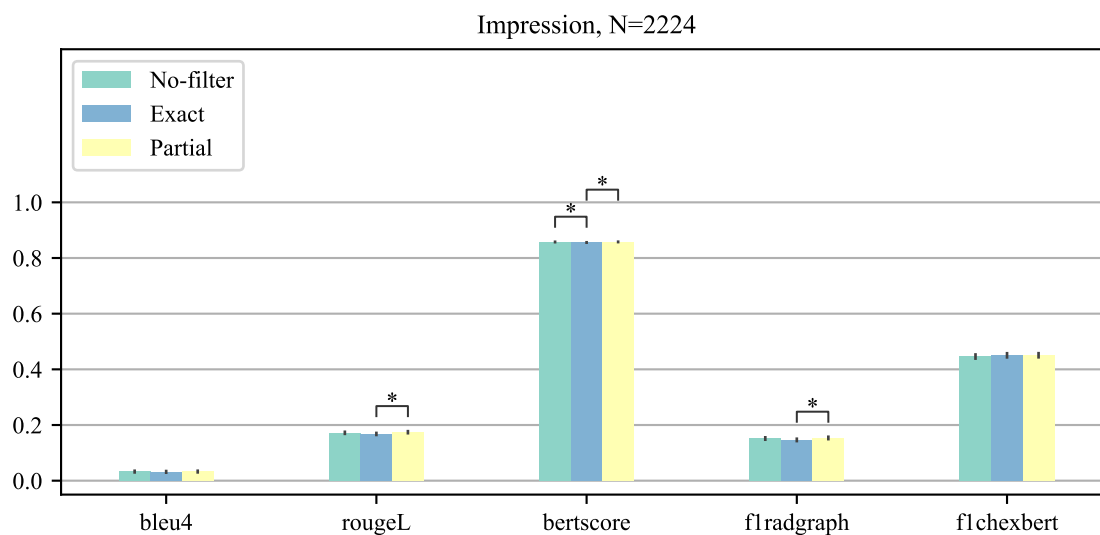
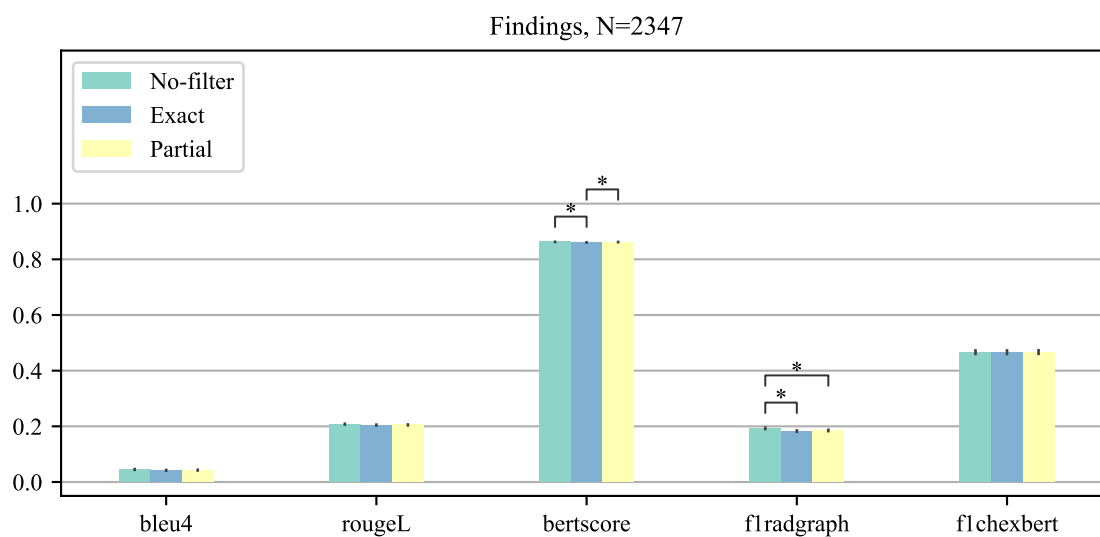


Figure S5. Comparison of LaB-RAG label filters. Significantly different pairs by paired t-test annotated if $p < 0.05$, Bonferroni correction applied for number of all pairwise comparisons per-plot. LaB-RAG otherwise defaults to “Simple” format/prompt, Mistral-v3, and predicted labels.

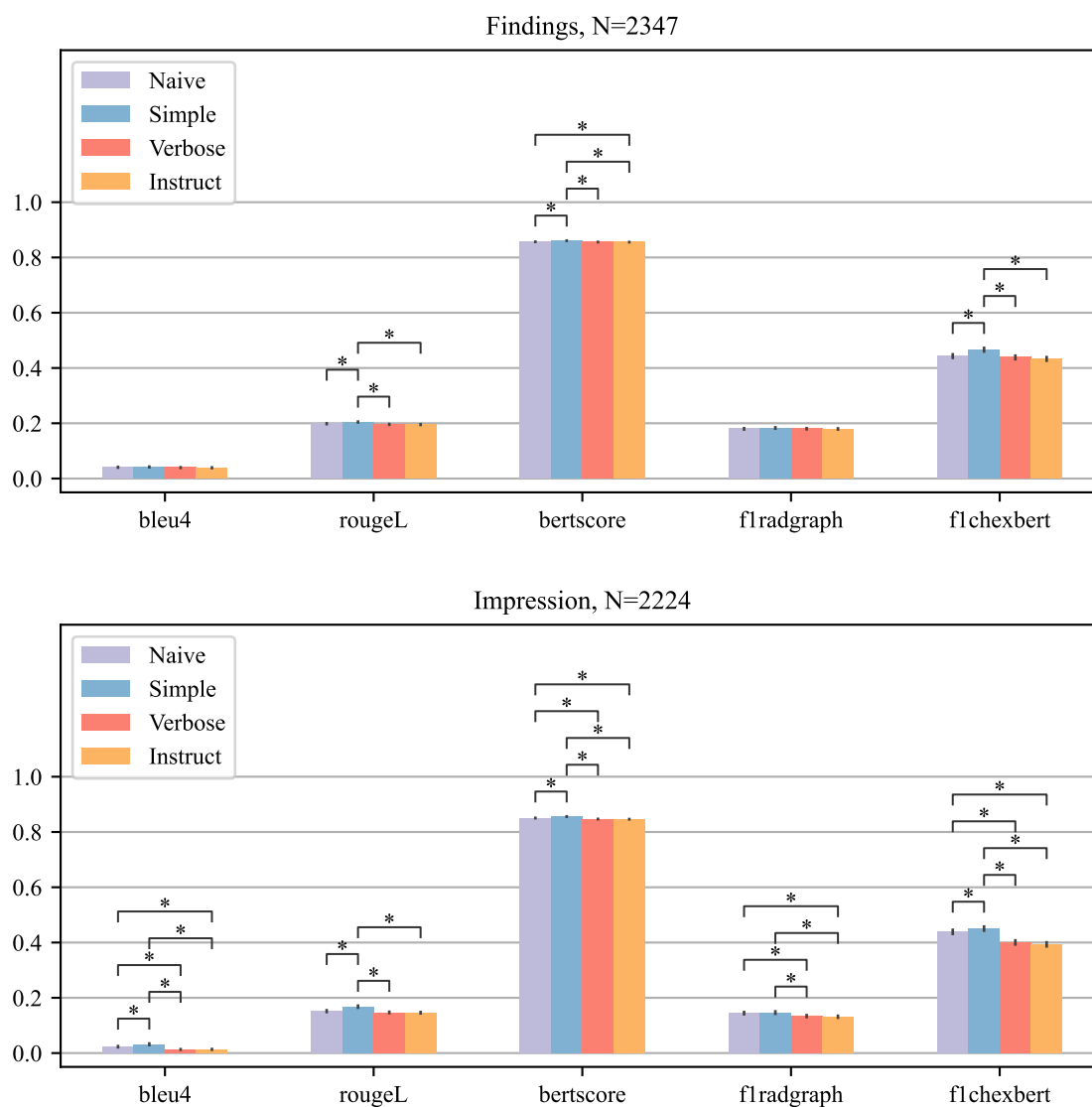


Figure S6. Comparison of LaB-RAG label formats. Significantly different pairs by paired t-test annotated if $p < 0.05$, Bonferroni correction applied for number of all pairwise comparisons per-plot. LaB-RAG otherwise defaults to “Exact” filter, Mistral-v3, and predicted labels.

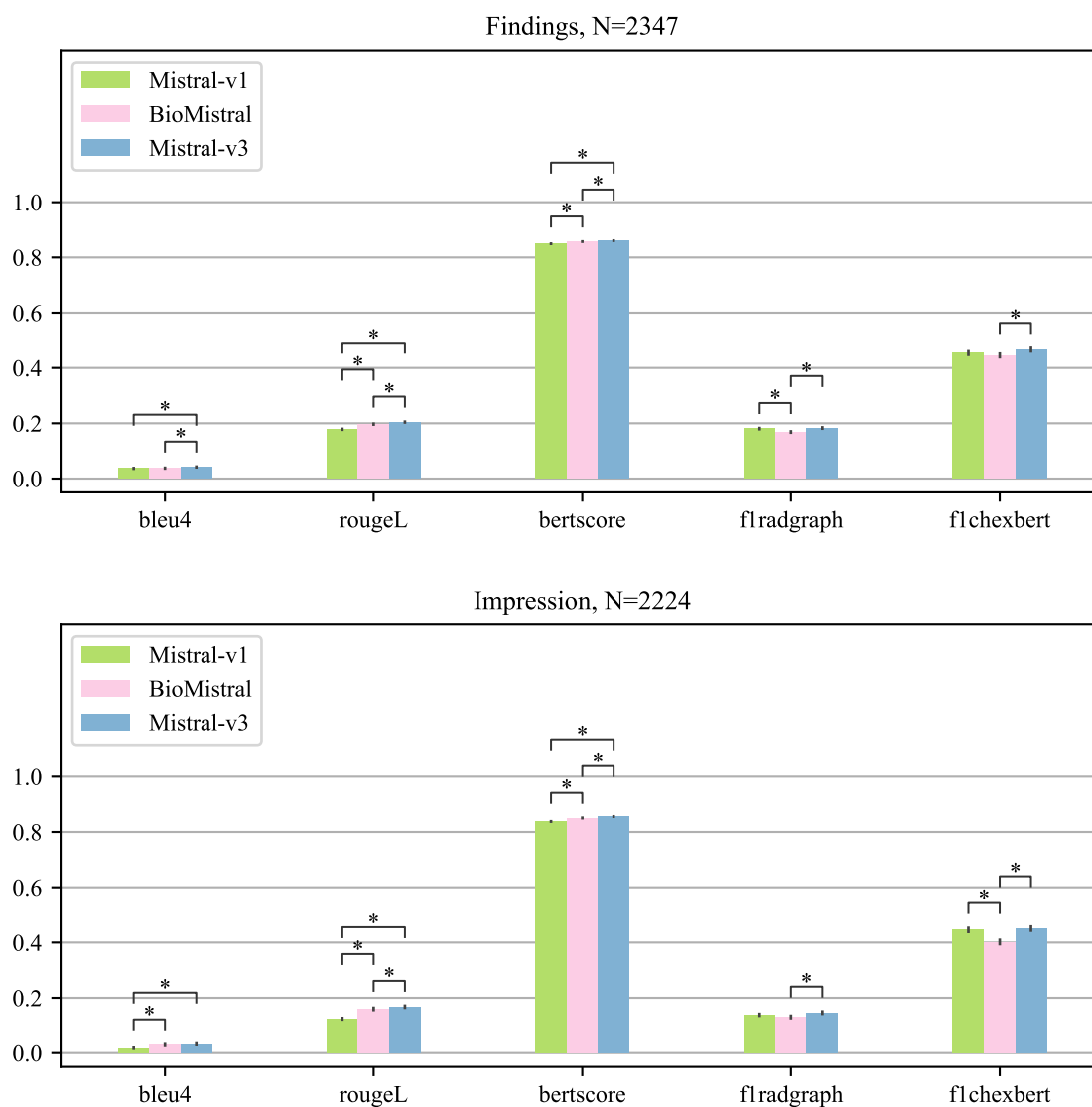


Figure S7. Comparison of different LLM modules for LaB-RAG. Significantly different pairs by paired t-test annotated if $p < 0.05$, Bonferroni correction applied for number of all pairwise comparisons per-plot. LaB-RAG otherwise defaults to “Exact” label filter, “Simple” format/prompt, and predicted labels.

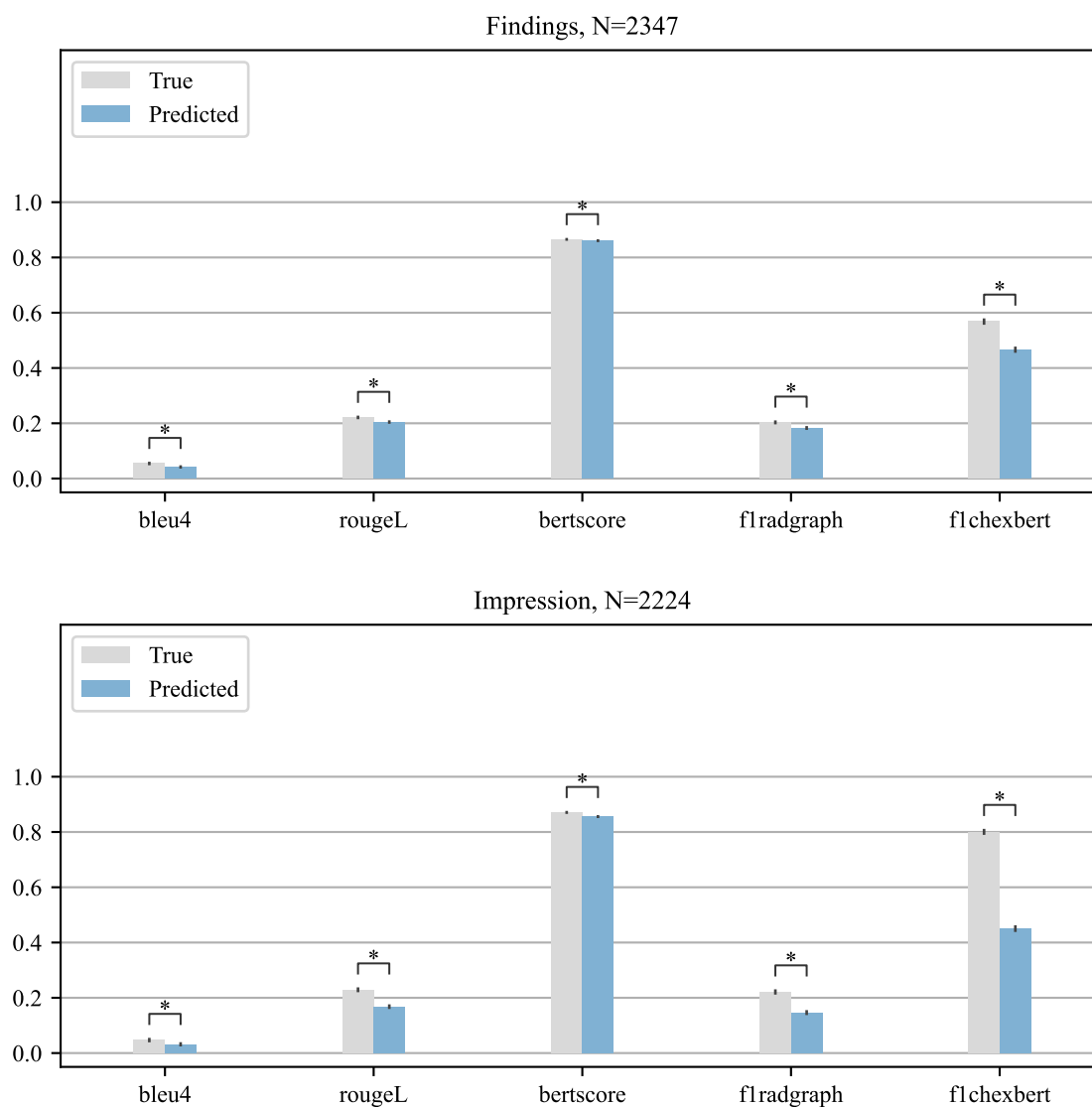


Figure S8. Comparison of label quality’s effect on LaB-RAG. Significantly different pairs by paired t-test annotated if $p < 0.05$, Bonferroni correction applied for number of all pairwise comparisons per-plot. LaB-RAG otherwise defaults to “Exact” format, “Simple” format/prompt, and Mistral-v3.

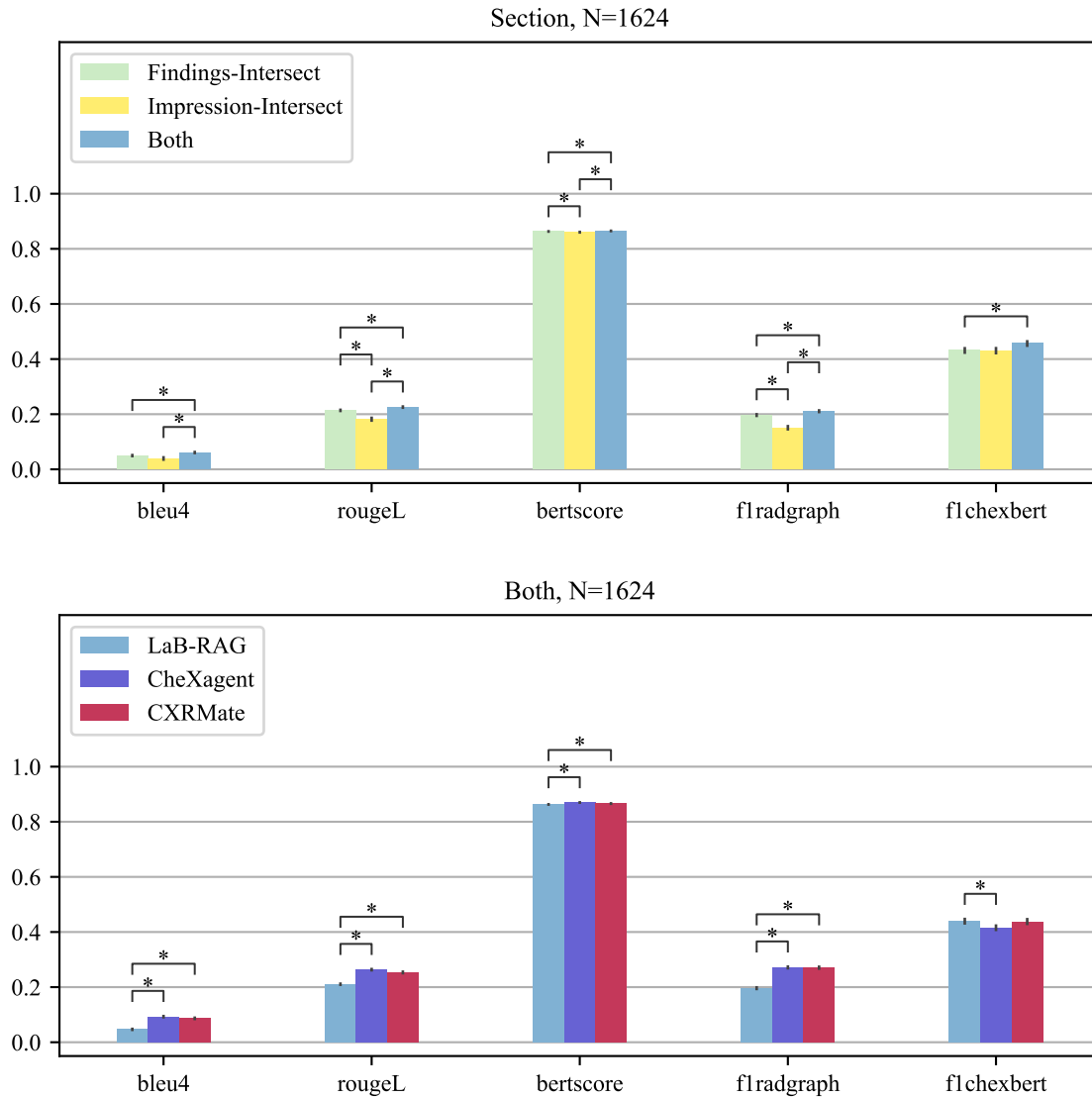


Figure S9. Comparison of generating different report sections and comparison of joint section generation against literature models. Significantly different pairs by paired t-test annotated if $p < 0.05$, Bonferroni correction applied for number of all pairwise comparisons per-plot. LaB-RAG otherwise defaults to “Exact” format, “Simple” format/prompt, Mistral-v3, and predicted labels.



Figure S10. Histogram of image similarity rank for top 5 studies selected for each inference image, after “Exact” label filtering or “Partial” label reordering. While similar images may share some labels with the inference image, they may not match exactly.